AD-A278 157

An Evaluation of Three GPS Receivers for Use in the GPS Sounder

DTIC
S ELECTE D
APR 1 3 1994
G

K. D. Anderson

94-11234

DTIC QUALITY INSPECTED 3
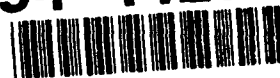
NRaD

Approved for public release; distribution is unlimited.

94 4 12 155

Technical Report 1637
April 1994

An Evaluation of Three GPS Receivers for Use in the GPS Sounder

K. D. Anderson

Accesion For		
NTIS CRA&I		☒
DTIC TAB		☐
Unannounced		☐
Justification		
By		
Distribution /		
Availability Codes		
Dist	Avail and / or Special	
A-1		

MA

SUMMARY

OBJECTIVE

The objective of this work is to evaluate the performance of geodetic quality Global Positioning System (GPS) receivers in support of the GPS Sounder task.

RESULTS

The signal processing and tracking capabilities of three GPS receivers were evaluated in severe multipath conditions. The Allen Osborne Associates (AOA) TurboRogue SNR-8000 is shown to be the receiver that is closest to meeting the requirements of the GPS Sounder task.

RECOMMENDATIONS

It is strongly recommended that the AOA TurboRogue SNR-8000 receiver be purchased to support the GPS Sounder task.

CONTENTS

TABLES

INTRODUCTION

Modern naval microwave communication and sensor system performance can be greatly affected by the spatial distribution of the refractive index in the lower atmosphere. A famous example of refractive effects on signal propagation is the WW II sighting of the Arabian coast with a 200-MHz radar from India 1700 miles away (Freehafer, 1951). Although a strong refractive gradient can confine an electromagnetic wave within a vertically thin layer such that over-the-horizon fields may be many tens of decibels higher than expected, conditions have been observed where radars could not detect a surface target that was optically visible (Freehafer, 1951).

In recent years, considerable effort has been put forth to create computer-based systems to assess refractive effects on signal propagation in the lower atmosphere (Hitney & Richter, 1976; Hitney et al., 1985). These assessment tools provide a near-realtime capability to evaluate the performance of radar and communication systems, and include tactical decision aids to mitigate or exploit atmospheric propagation effects. However, a crucial factor for these analysis tools is a thorough knowledge of the spatial distribution of refractivity.

Conventional direct atmospheric sensing by radiosondes or airborne microwave refractometers is inconvenient and expensive. In addition, these sensors measure the refractivity in a limited volume of space. A radiosonde rising through the atmosphere only measures refractivity along the line of its ascent. Although typical correlation scales for refractivity are tens of kilometers in the horizontal, tens of meters in the vertical, and hours in time, typical propagation problem scales are tens to hundreds of kilometers in the horizontal, 1 to 10 kilometers in the vertical, and hours in time. Generally, without additional radiosonde or refractometer measurements, horizontal homogeneity in the refractive structure is a necessary assumption.

The Global Positioning System (GPS) Sounder task will develop techniques to infer the vertical refractive profile of the lower atmosphere from ground-based measurements of GPS satellite signals as the GPS satellite rises or sets on the horizon. There are obvious advantages to this concept. First, the inferred profiles will be representative of the integrated refractive effects along the range–height path instead of a single time and space line representation of refractivity. Second, with the completion of the GPS constellation, there will be at most 84 times per day when a GPS satellite will rise or set on the horizon. A receiver located near the equator will see rise and set locations nearly uniformly distributed in azimuth. As the receiver latitude approaches either pole, there will be fewer and fewer rise and set locations in the direction of the pole. Figure 1 shows a polar plot of the GPS satellite tracks seen at the Naval Command, Control Ocean Surveillance Center, RDT&E Division (NRaD) Bldg. 323 test site for one 24-hour period. The projection is in terms of zenith angle and azimuth.

A third advantage to this concept is the leveraging of a multibillion dollar system that is fully functional. The satellites are in place, the signal structure is well known, the hardware is mature, and the receivers are commercially available. Lastly, the concept is one that can easily be automated. Ideally, a GPS receiver and a small computer are all that is needed for processing. A microcomputer has the computational horsepower to control the receiver, process the data, infer the profile, and even transfer the profile to propagation assessment computer systems.
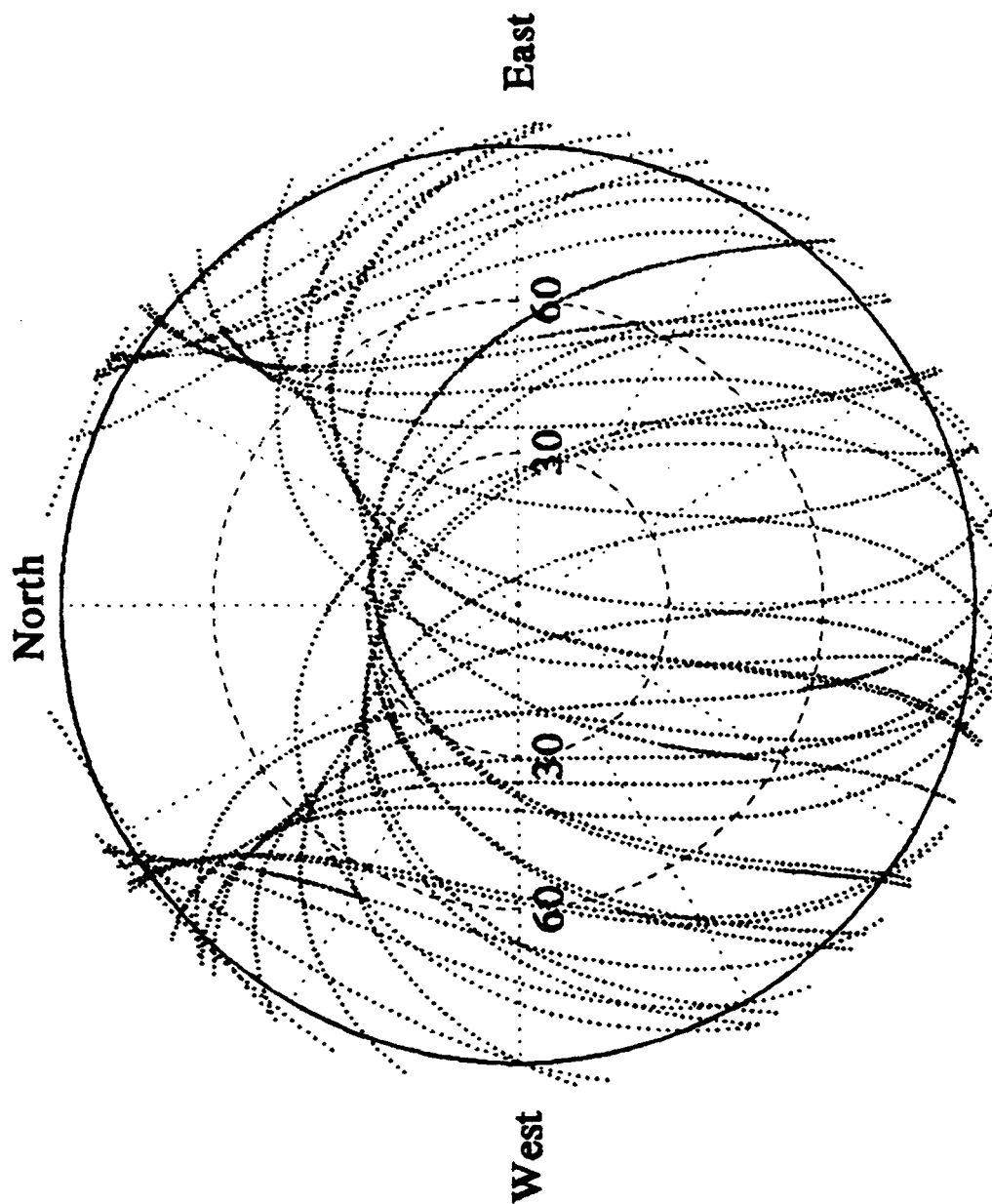
1

Figure 1. Typical satellite coverage, NRaD Bldg. 323.

2

The GPS Sounder is a fresh look at the problem of inferring the refractive profile from monitoring satellite signals as described by Anderson (1982) and patented by Hitney (1978). With the assumption that the received signal is the sum of a direct ray and a sea-reflected ray, as illustrated by figure 2, the elevation angle of the direct ray is related to the path length difference δ between the direct and reflected ray. As the satellite moves through its orbit, δ changes many wavelengths. When δ is an integral number of wavelengths, the received signal level is a minimum, or null, because there is a phase shift of π radians upon reflection at the surface. When δ is an integral number of wavelengths plus a half a wavelength, the direct and sea-reflected rays are in phase and the voltage at the receiver is a maximum or interference peak.

The upper plot of figure 3 shows the modeled and observed interference pattern (Lloyd's Mirror effect) where the abscissa is ground range to the satellite and the ordinate is propagation loss. The observed data (light curve) are from a set of measurements made on 20 July 1978 at NRaD (Anderson, 1982) using signals from the *Wideband* satellite. The transmission frequency was 1239 MHz and the satellite was in a nominal 1000-km polar orbit. The modeled interference pattern (connected solid circle symbol curve) is derived from the refractivity profile measured at the receiver site using a radiosonde and a unique propagation model (Hitney, 1993) that combines ray optic and parabolic equation-solving methods to evaluate the wave equation for propagation on satellite-to-ground paths. At the closest subsatellite ranges (highest elevation angles), the predicted and observed interference pattern are in excellent agreement. At the farthest subsatellite ranges, the patterns are different. The bottom plot on figure 3 is a range–height diagram of propagation loss for the same case. Small changes in the refractivity profile 70 to 80 km down range from the receiver could have a large effect on the stretching or contraction of the interference pattern at long subsatellite ranges. Unfortunately, the refractive conditions at these distances were not measured in 1978. However, the data displayed in figure 3 clearly show there are reasonable possibilities of estimating the effective refractive profile from RF measurements along a satellite-to-ground path.

In 1978, the measurement equipment needed to monitor and record the *Wideband* satellite signals occupied three racks. Today, high performance, multichannel, GPS receivers are smaller than a brief case and are readily available. The problem of selecting a GPS receiver for the GPS Sounder task is that the manufacturers' specifications are almost exclusively related to geodetic capabilities where the satellites are generally well above the horizon. A preliminary market survey of equipment manufacturers was conducted in early summer of 1993. From this survey, three manufacturers responded with equipment that could be usable with the GPS Sounder. The manufacturers and equipment are listed in table 1. Allen Osborne Associates, Inc. (AOA) and Trimble Navigation Ltd. graciously loaned their equipment free of charge for testing at NRaD. Ashtech, Inc. agreed to rent their equipment for a nominal fee. All three companies provided excellent technical support during the tests.

Table 1. GPS receivers used in tests.

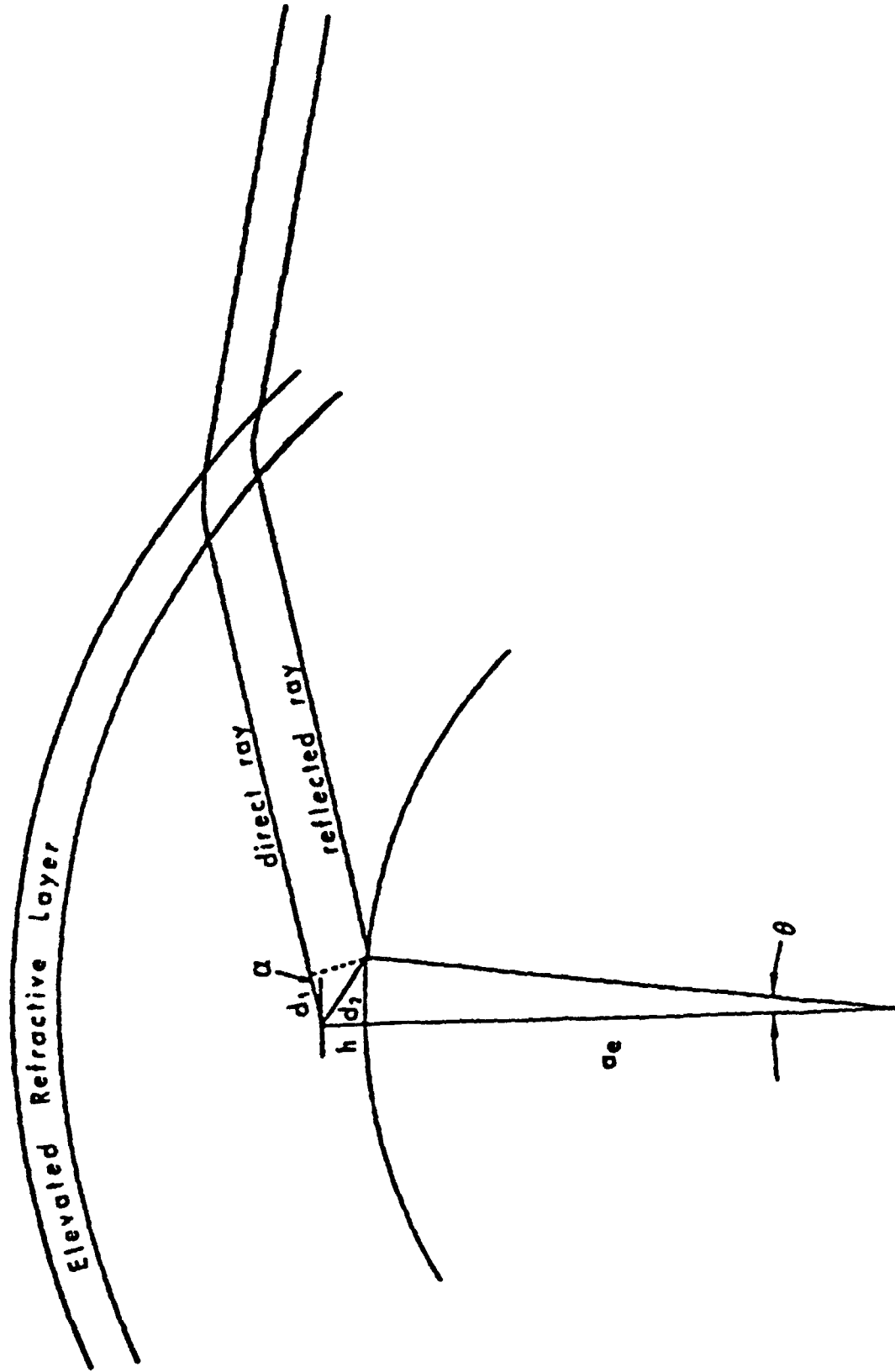| Company	Equipment	Firmware
Allen Osborne Associates	TurboRogue SNR-8000	1.1c
Trimble Navigation	4000SSE	Nav5.64, Sig1.23, Boot3.30
Ashtech	MD XII C	ChVer66, NavVer7A CapL2C

3

Figure 2. Satellite-to-ground ray path geometry. Path length difference between the direct and the ray is defined as $d_1 - d_2$.
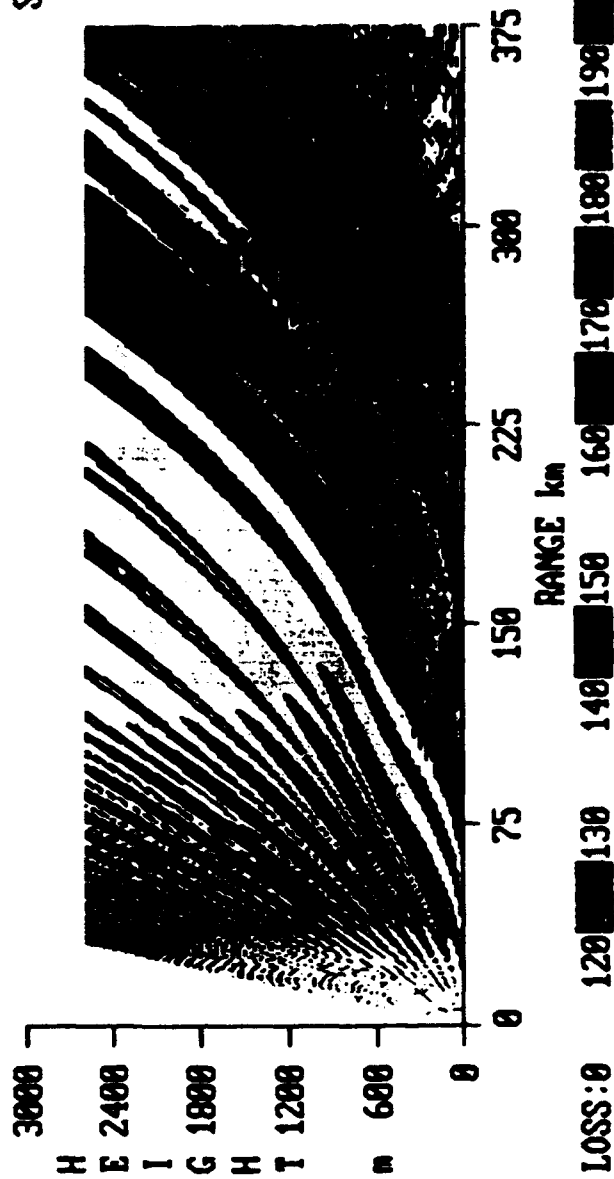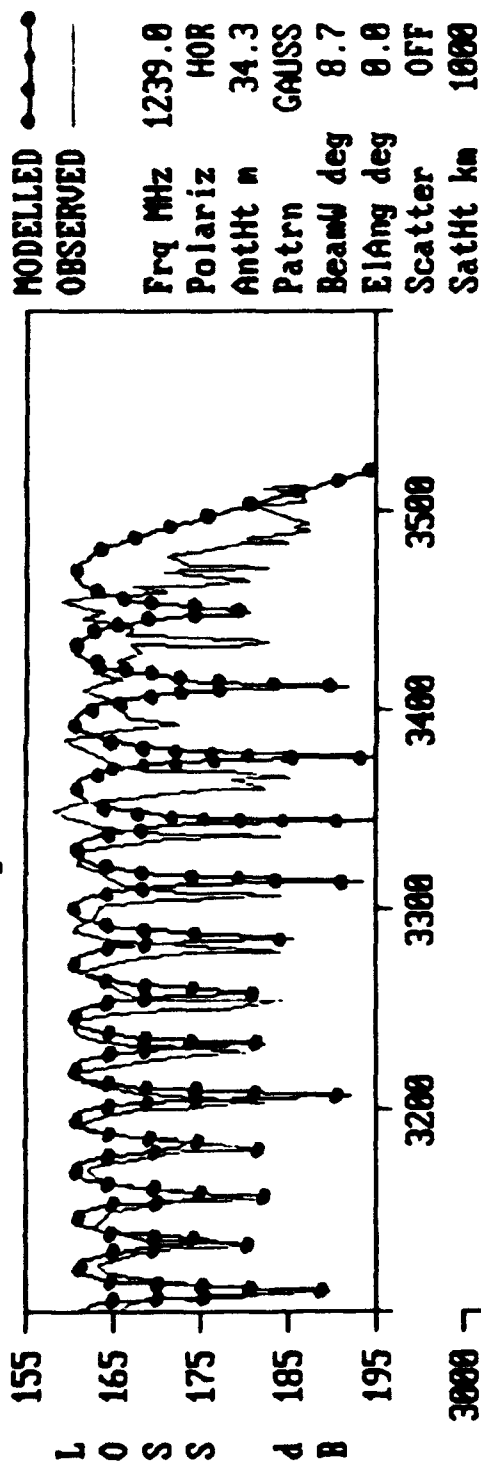
4

Figure 3. Modeled and observed signal interference pattern for a measurement made on 28 July 1978.

MEASUREMENTS AND RESULTS

The measurements were conducted at NRaD, Bldg. 323, during the month of August 1993. The test site is located at lat 32°41'47.89561"N, long 117°15'12.42723"W, with the antenna located at an orthometric height of 42.00 ± 0.05 m (6.81 ± 0.05 m above the ellipsoid). This facility overlooks the Pacific Ocean. There is an unobstructed view of the ocean horizon for azimuth angles from about 180 to 350 degrees. The GPS receiver antenna, supplied by each manufacturer, was tilted about 15 degrees downward toward the west to reduce the effect of multipath signal reduction designed into some of the antennas (AOA supplied a choke ring antenna). Each receiver was computer-controlled and programmed to report raw data, signal-to-noise ratio (SNR) and carrier phase at 1-second intervals. The satellite elevation mask angle for the AOA and the Trimble units was set negative, typically –5 or –10 degrees. The Ashtech unit would not accept a negative mask angle and it was set to 0 degree (Ashtech technical support indicated that the unit should be able to track satellites to negative elevation angles). For a data collection period when a satellite was rising or setting on the horizon, each receiver was pro-grammed to enable that satellite and 4 to 6 other satellites that were at high angles. The tracking of these additional 4 to 6 satellites appeared to be necessary so the receiver could lock onto good signals and determine location, which seemed to be required by the firmware. As the desired satellite rose or set, each receiver internally logged the data. None of the receivers could report the raw data (in ASCII format) in realtime using the serial port. The internal firmware could not keep up with the 1-second update rates and the amount of raw data (the amount varied according to the manufacturer). The internal data were off-loaded from the receiver after the recording session.

Table 2 summarizes the measurement periods that began on 10 August 1993 and ended on 25 August 1993. There was 1 day of measurements with the AOA receiver (10 August 1993) with four satellites rising or setting (satellites 17, 25, 12, and 22). There were 3 days of measurements using the Trimble receiver (19, 20, and 22 August). Measurements with the Ashtech receiver were made on 25 August. In table 2, the column labeled "# of satellites locked" indicates how many additional satellites were enabled and locked on during the test period. Data in the columns labeled "predicted rise/set time" and "rise/set azimuth degrees" were derived from files of pre-cise orbital positions that were obtained from the National Geodetic Service (NGS), Rockville, MD. The rise or set time is defined as the epoch when the geometric elevation angle from the receiver position to the satellite is 0 degree. The last column in table 2 is the geometric elevation angle at the epoch, either when the receiver first sensed the rising GPS satellite or when the receiver last sensed the setting GPS satellite.

ALLEN OSBORNE ASSOCIATES TURBOROGUE SNR-8000

Figures 4 through 7 are the SNR measurements for the C/A, P1, and P2 code loops extracted as the raw data from the AOA receiver. C/A and P1 are transmitted on the same frequency, L1, at 1575.42 MHz. P2 is transmitted on a lower frequency, L2, at 1227.60 MHz. In these figures, the interference pattern is readily observable for elevation angles greater than about 1 degree. At angles lower than about 1 degree, only portions of the pattern are observed. This is expected as the digital lock loop breaks lock when no signal is present (in a null) and reacquires the signal sometime after the signal has exceeded an SNR threshold enabling the loop to lock. For the rising satellites, 17, 25, and 22 (figures 4, 5, and 7), the "half pattern" is toward higher elevation

6

angles. For the setting satellite, 12 (figure 6), the "half pattern" is toward the lower elevation angles.

Table 2. Summary of GPS receiver measurements.

Day Aug 1993	Receiver & Data Set #	PRN	Data Start Time (GMT)	Data End Time (GMT)	# of Satellites Locked	Predicted Rise/Set Time	Rise/Set Azimuth Degrees	Minimum Elevation Angle Observed
10	AOA 1	17	18:44:08	19:19:37	5	18:56:02 Rise	226	−0.95
10	AOA 1	25	18:44:08	19:19:37	5	18:56:26 Rise	326	−1.80
10	AOA 2	12	20:33:44	21:10:47	4	20:42:14 Set	192	−0.20
10	AOA 2	22	20:33:44	21:10:47	4	20:57:32 Rise	325	−1.20
19	Trimble 3	28	22:10:45	22:32:05	4	22:12:25 Rise	318	+0.20
20	Trimble 4	20	16:17:42	16:47:50	4	16:21:28 Rise	304	−1.10
20	Trimble 4	26	16:17:42	16:47:50	4	16:25:49 Set	216	−0.55
22	Trimble 5	20	15:50:23	16:38:51	4	16:13:24 Rise	304	−0.50
22	Trimble 5	26	15:50:23	16:38:51	4	16:17:34 Set	216	−0.75
25	Ashtech 7	20	15:37:33	16:18:45	5	16:01:18 Rise	304	+0.40
25	Ashtech 7	26	15:37:33	16:18:45	5	16:05:11 Set	216	−0.20
25	Ashtech 8	22	19:30:03	20:27:32	5	19:56:57 Rise	325	+1.84
25	Ashtech 8	23	19:30:03	20:27:32	5	19:33:12 Rise	204	+2.22
25	Ashtech 8	25	19:30:03	20:27:32	5	20:19:49 Set	268	−0.01

In figure 4, a null in both L1 and L2 occurs at an elevation angle of 2.7 degrees. At this point, the path length difference between the direct and sea-reflected rays must be an integer number of wavelengths. This fact can be used to eliminate the phase ambiguity. The frequency ratio of L1 to L2 is 154:120, so the ratio of the wavelengths is 120:154. In figures 5 and 6, the cofrequency null location is at an elevation angle of about 2.69 degrees; slightly less than in figure 4. In figure 7, the cofrequency null location is at about 2.72 degrees; slightly greater than in figure 4. The change in the elevation angle of the cofrequency null location may be due to spatial and temporal changes in the refractivity profile.

AOA TurboRogue SNR 8000
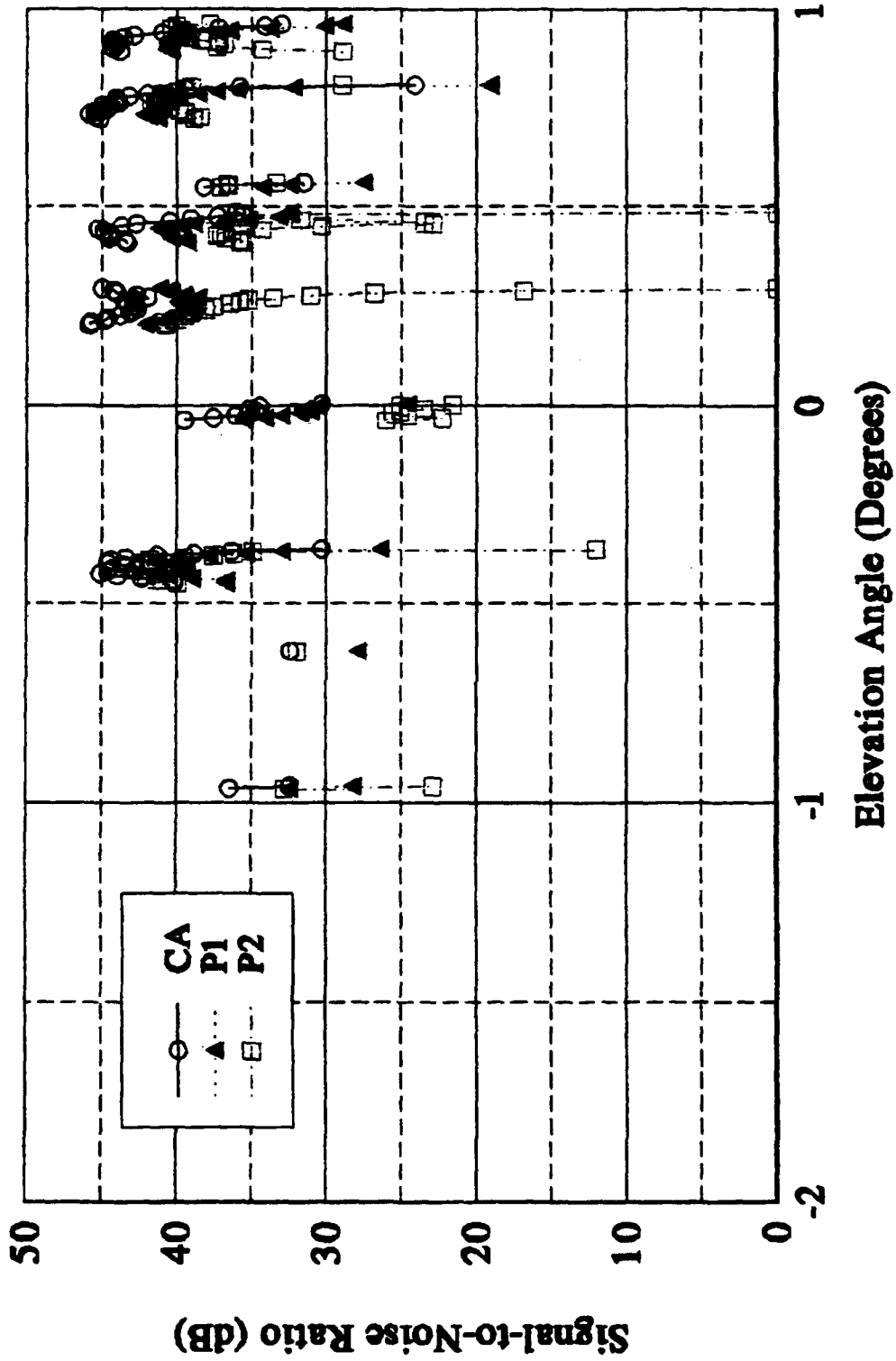**10 August 1993, Satellite 17, 226 Degrees**

Signal-to-Noise Ratio (dB)

Elevation Angle (Degrees)

CA
P1
P2

Figure 4a.   SNR for satellite 17 rising on 10 August 1993 as measured by the AOA TurboRogue receiver.

8

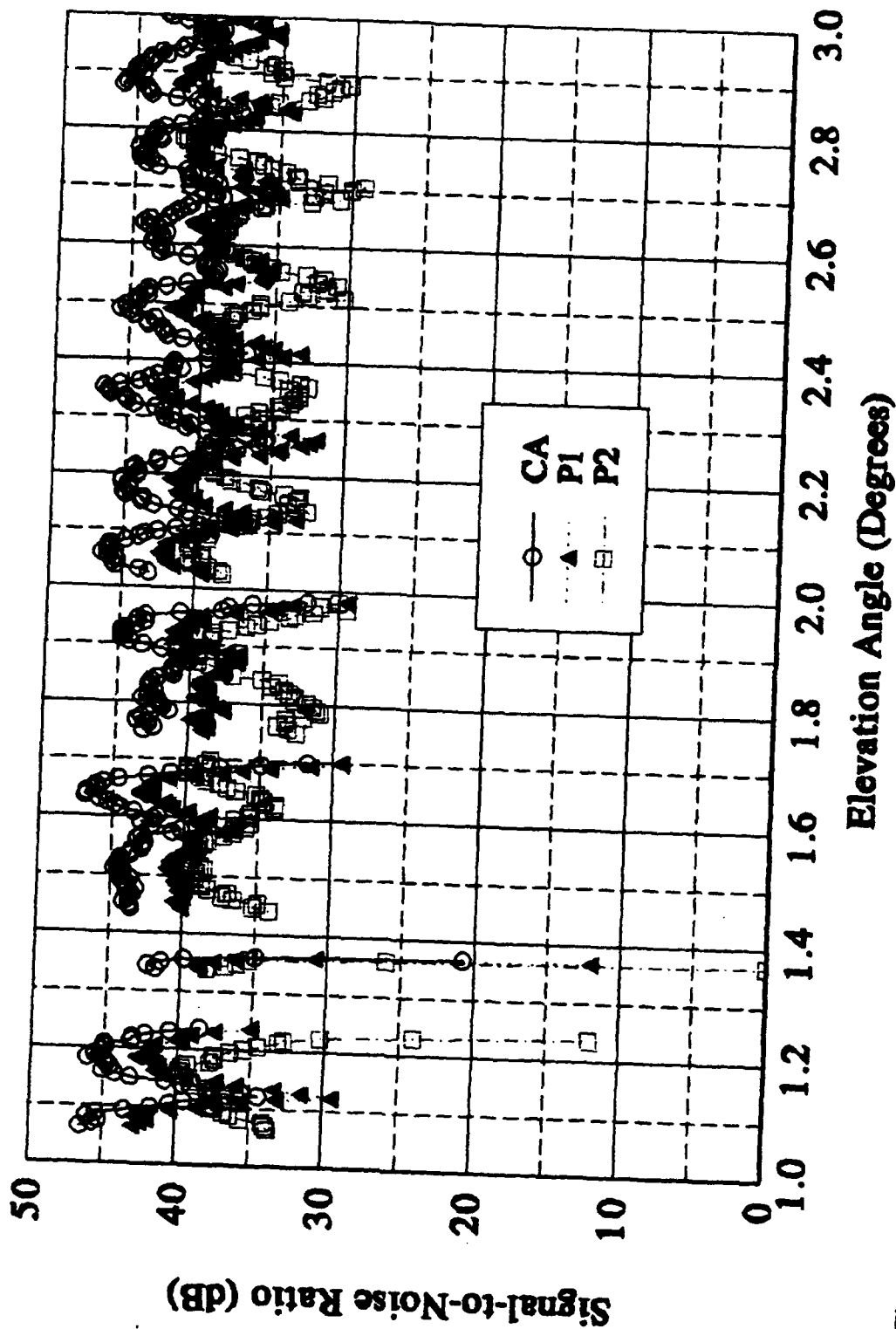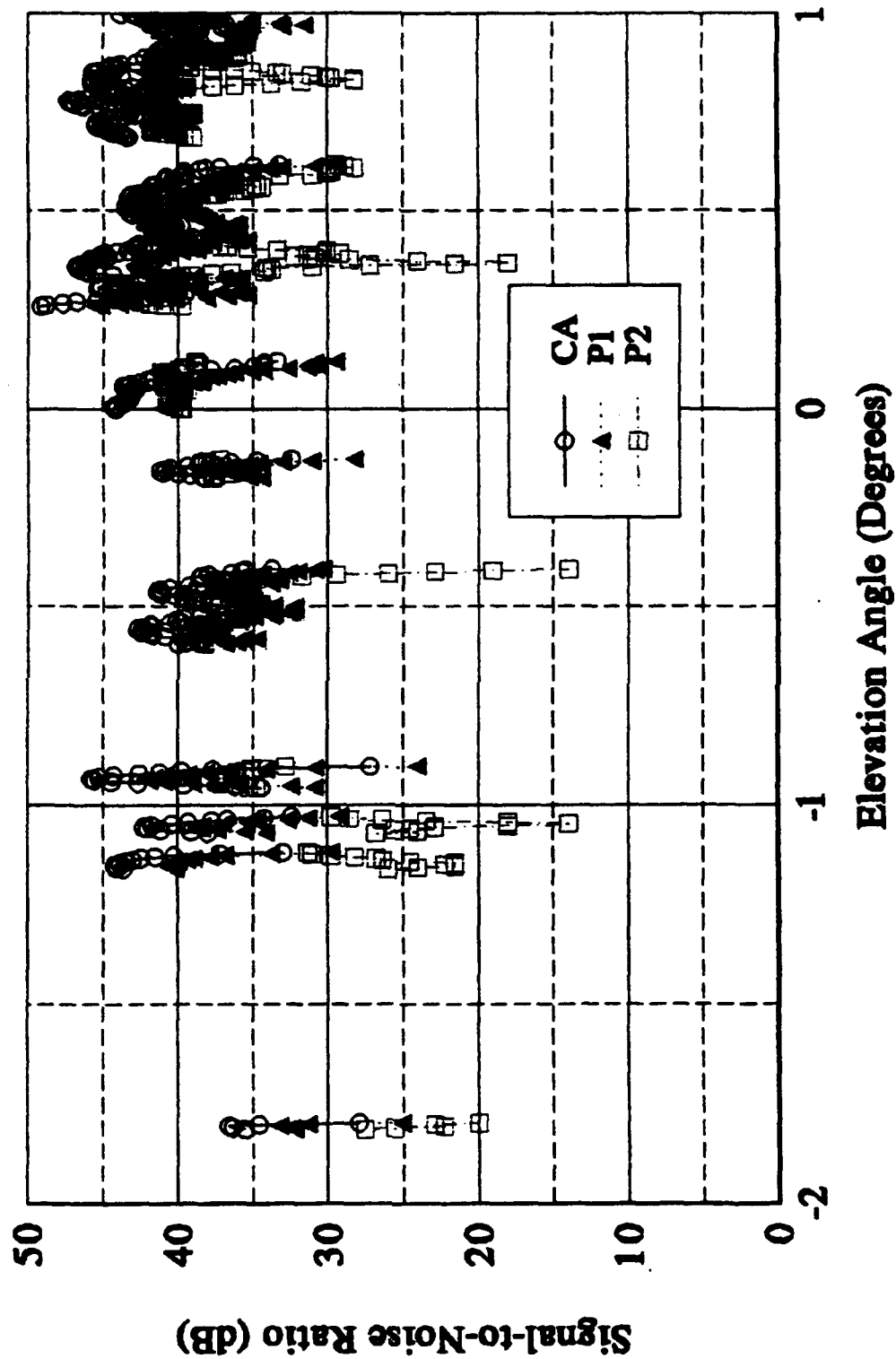**AOA TurboRogue SNR 8000**
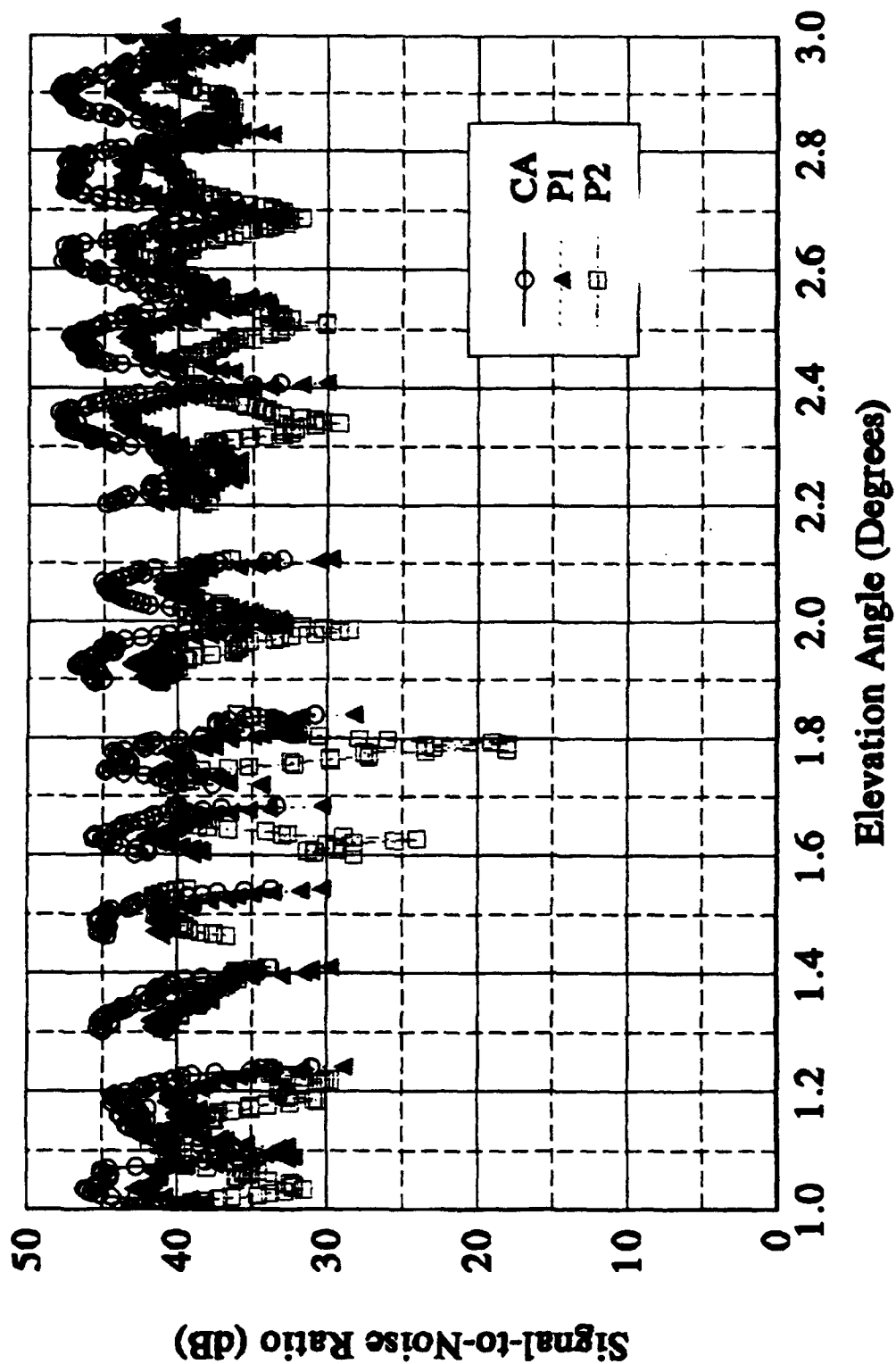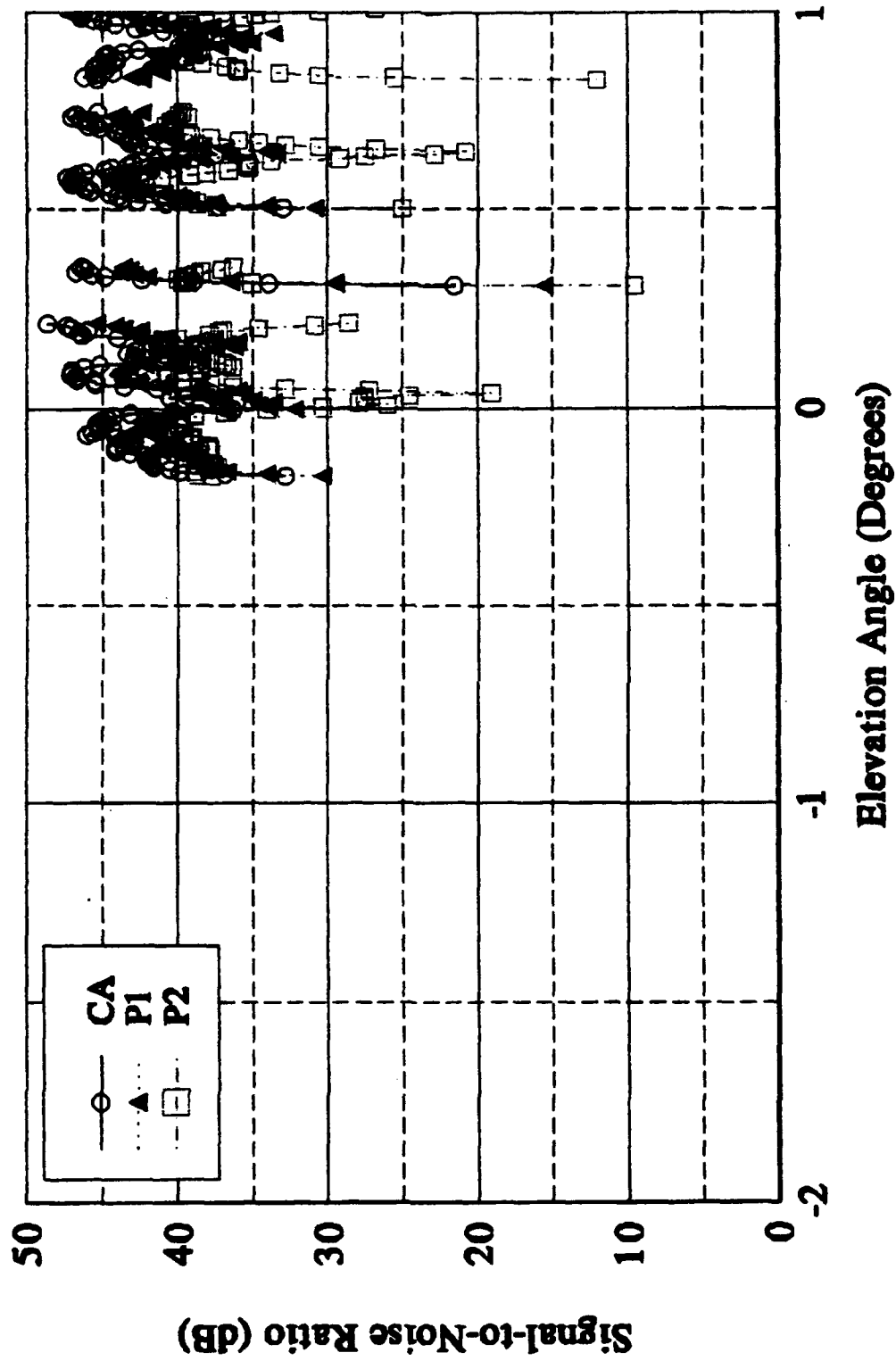10 August 1993, Satellite 17, 226 Degrees

Signal-to-Noise Ratio (dB) vs. Elevation Angle (Degrees)
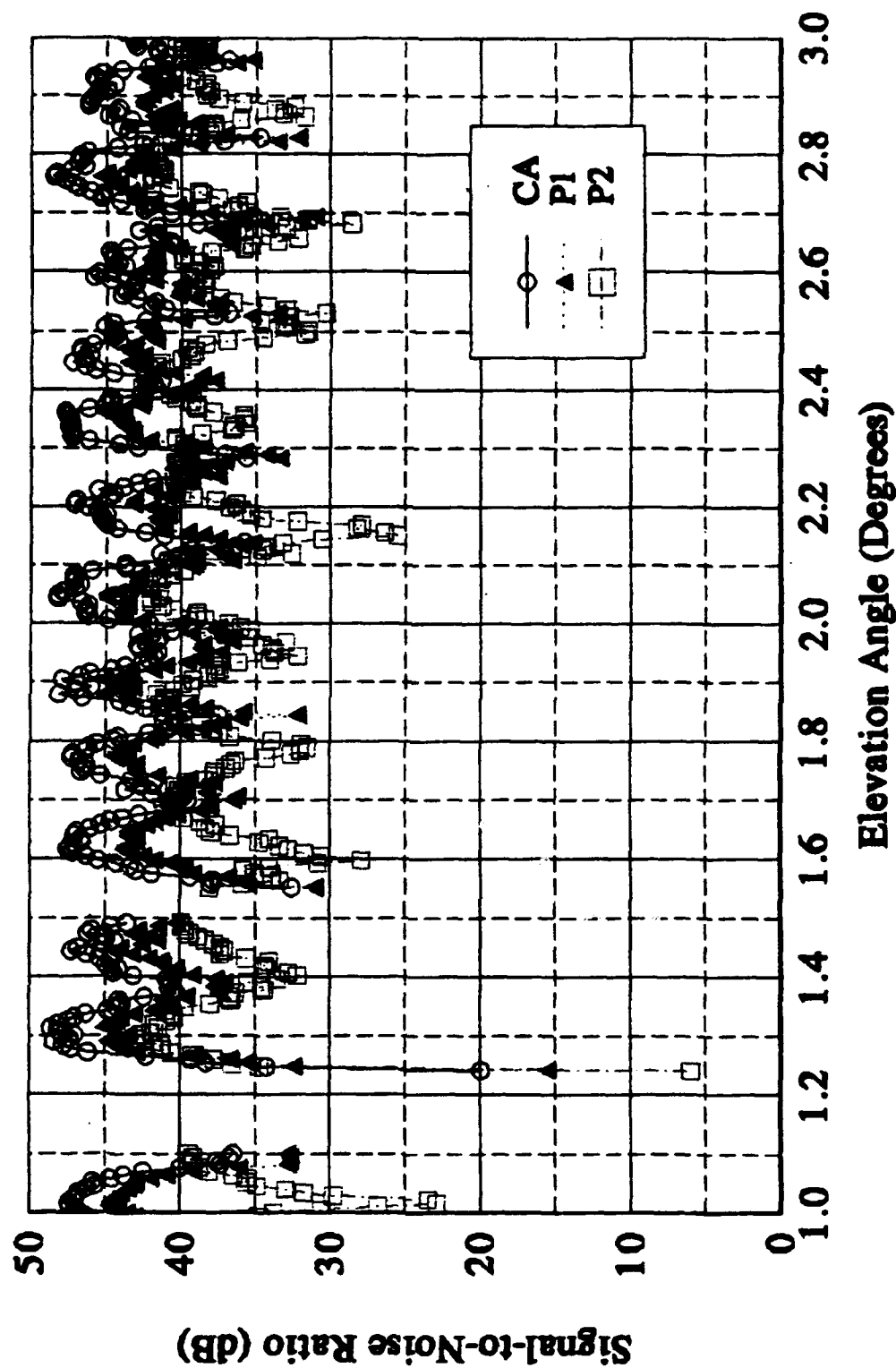
Legend: CA, P1, P2

Figure 4b.   SNR for satellite 17 rising on 10 August 1993 as measured by the AOA TurboRogue receiver (cont'd).

9

AOA TurboRogue SNR 8000
10 August 1993, Satellite 25, 326 Degrees

Signal-to-Noise Ratio (dB)

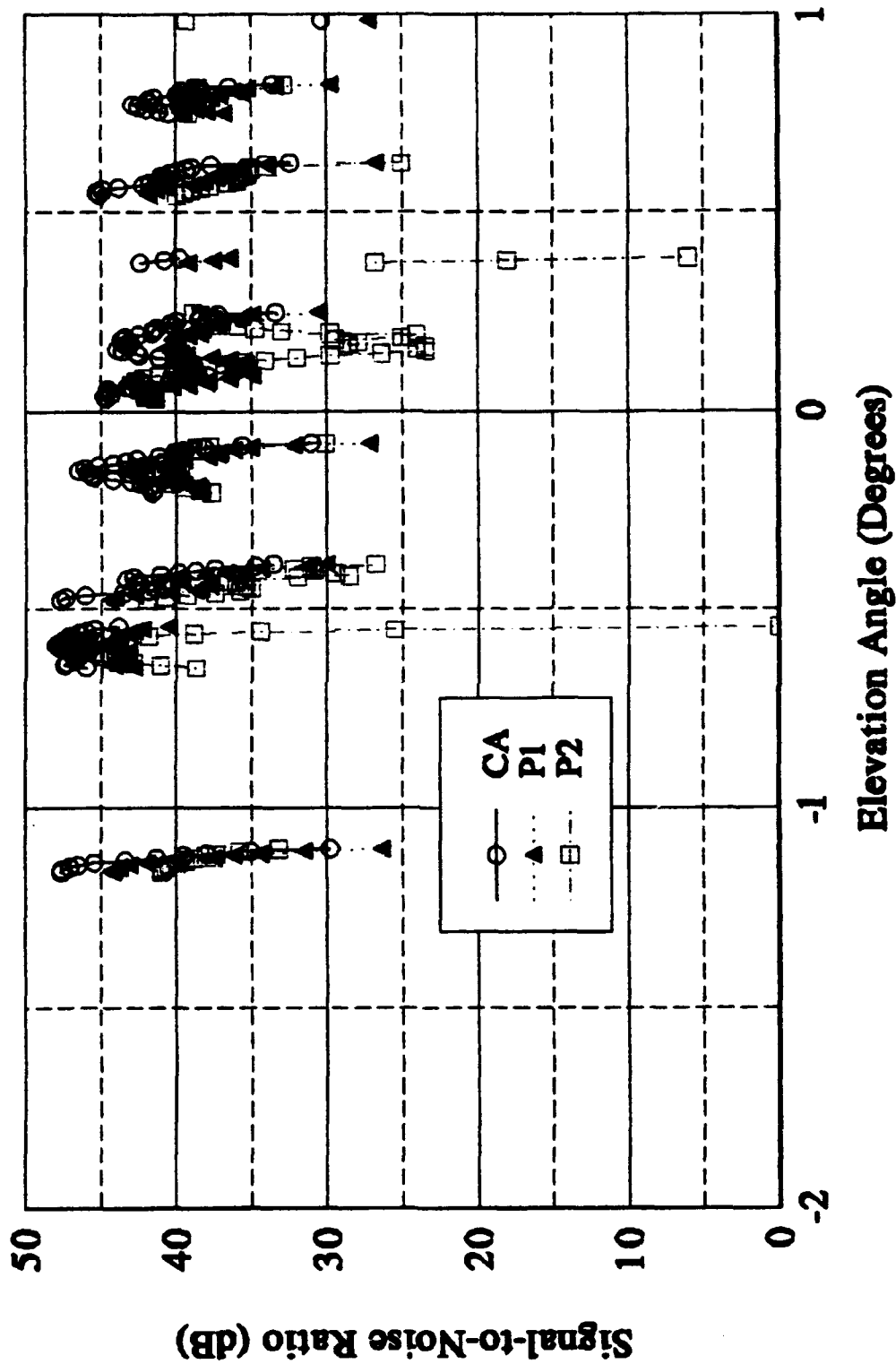**Elevation Angle (Degrees)**

Legend:
- CA
- P1
- P2

Figure 5a. SNR for satellite 25 rising on 10 August 1993 as measured by the AOA TurboRogue receiver.

10

AOA TurboRogue SNR 8000
10 August 1993, Satellite 25, 326 Degrees

Signal-to-Noise Ratio (dB)

Elevation Angle (Degrees)

CA
P1
P2

Figure 5b. SNR for satellite 25 rising on 10 August 1993 as measured by the AOA TurboRogue receiver (cont'd).

11

AOA TurboRogue SNR 8000
10 August 1993, Satellite 12, 192 Degrees

Legend: CA, P1, P2

X-axis: Elevation Angle (Degrees)

Y-axis: Signal-to-Noise Ratio (dB)

Figure 6a. SNR for satellite 12 setting on 10 August 1993 as measured by the AOA TurboRogue receiver.

12

AOA TurboRogue SNR 8000
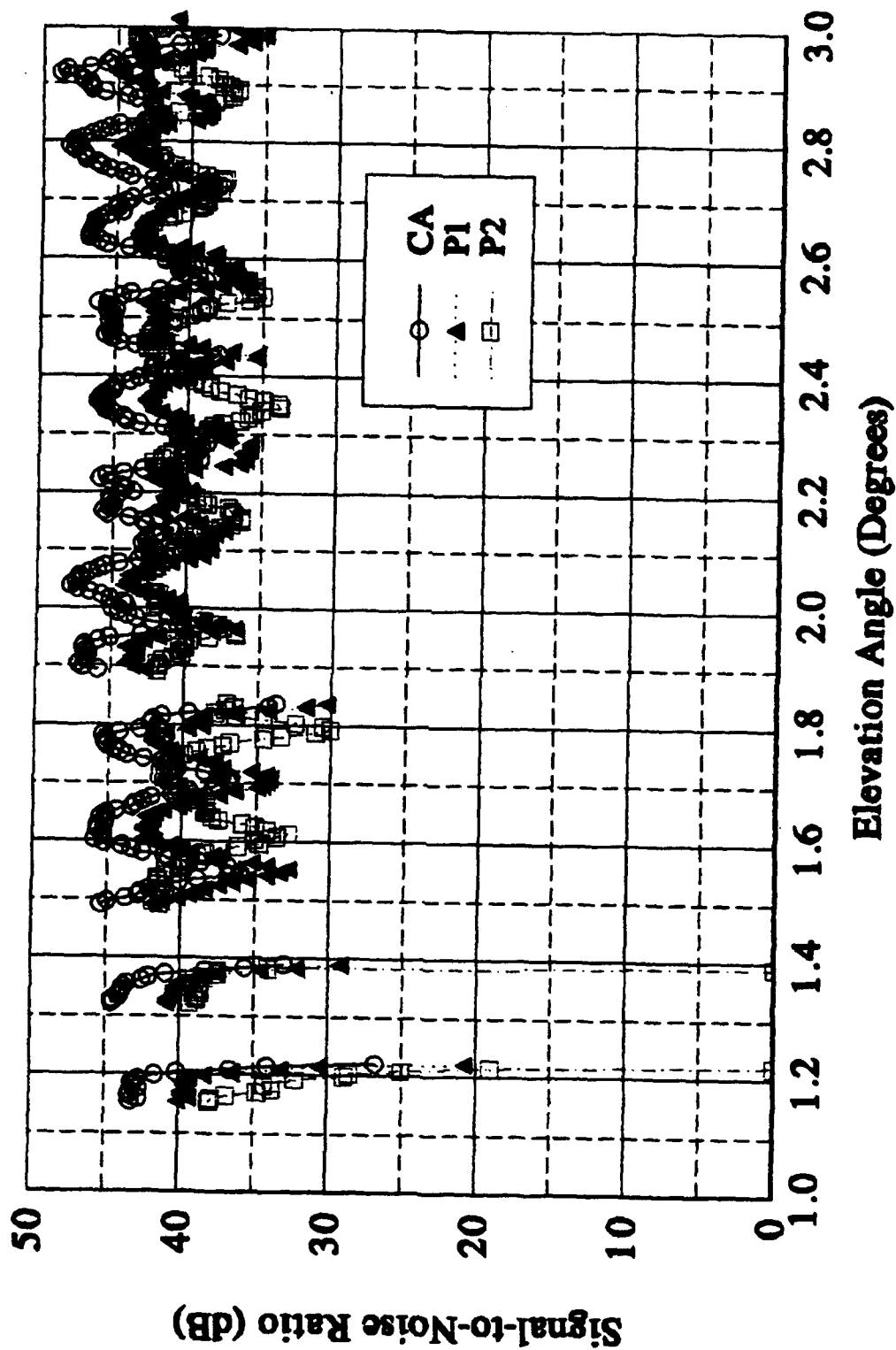**10 August 1993, Satellite 12, 192 Degrees**

Figure 6b. SNR for satellite 12 setting on 10 August 1993 as measured by the AOA TurboRogue receiver (cont'd).

13

Figure 7a.   SNR for satellite 22 rising on 10 August 1993 as measured by the AOA TurboRogue receiver.

14

Figure 7b. SNR for satellite 22 rising on 10 August 1993 as measured by the AOA TurboRogue receiver (cont'd).

TRIMBLE NAVIGATION 4000 SSE

Measurements using the Trimble 4000 SSE are shown in figures 8 through 12. The raw SNR data from uis unit are expressed in counts and are plotted as decibels relative to one count for comparison to the AOA data. On L1, the Trimble unit first acquires the C/A code then switches to track the P1 code. The raw data carry additional control bits to indicate whether C/A or P1 code is processed. Comparing these data to the AOA data, it is evident that the extraction of the interference pattern from the Trimble data is much more difficult. It appears that the Trimble lock loops are not as responsive as the AOA loops.

In addition, the P2 (L2) data are, in some cases, sparse, making identification of the cofrequency null location difficult if not impossible.

ASHTECH MD XII

The Ashtech MD XII receiver monitors only P code. C/A code processing is not available, but this would not be significant if both P codes were readily available. The results from the MD XII test are shown in figures 13 through 17. Like the Trimble unit, the raw data SNR for the P code loops are expressed in counts. Unlike the Trimble unit, the dynamic range of the P2 loop is small, ranging from 0 to 10 in integer steps. The P1 code loop clearly shows the interference pattern but the receiver does not seem to be able to lock onto the signal at negative elevation angles.

In only two of five cases does the Ashtech receiver track the satellite at geometric elevation angles less than 0 degree; even then, the elevation angles are comparatively close to 0 degree (-0.01 and -0.20 degree). In two cases the Ashtech receiver was not able to lock onto the satellite until the satellite had risen to well above one degree. For all five of the Ashtech measurements, the receiver start and end times bracketed the predicted rise/set time. The failure to lock onto the satellites at low and negative elevation angles appears to be associated with receiver processing and not external events or conditions. An earlier analysis by Rocken and Meertens (1992) also indicates that the Ashtech receiver does not lock and track at very low elevation angles.

The local refractive conditions, measured with radiosondes launched near the test site, while not identical between days and tests, were similar during the entire August measurement period. Generally, the refractive conditions could be described as an elevated duct with a base at about 200 m and a top at about 600 m. It is unlikely that the slightly different refractive conditions during the Ashtech measurement period are responsible for the receiver not locking onto the satellite until the elevation angle is at or above 0 degree.

THIS PAGE INTENTIONALLY LEFT BLANK

Trimble 4000 SSE
19 August 1993, Satellite 28, 318 Degrees

Signal-to-Noise Ratio (Units)

Elevation Angle (Degrees)

Legend:
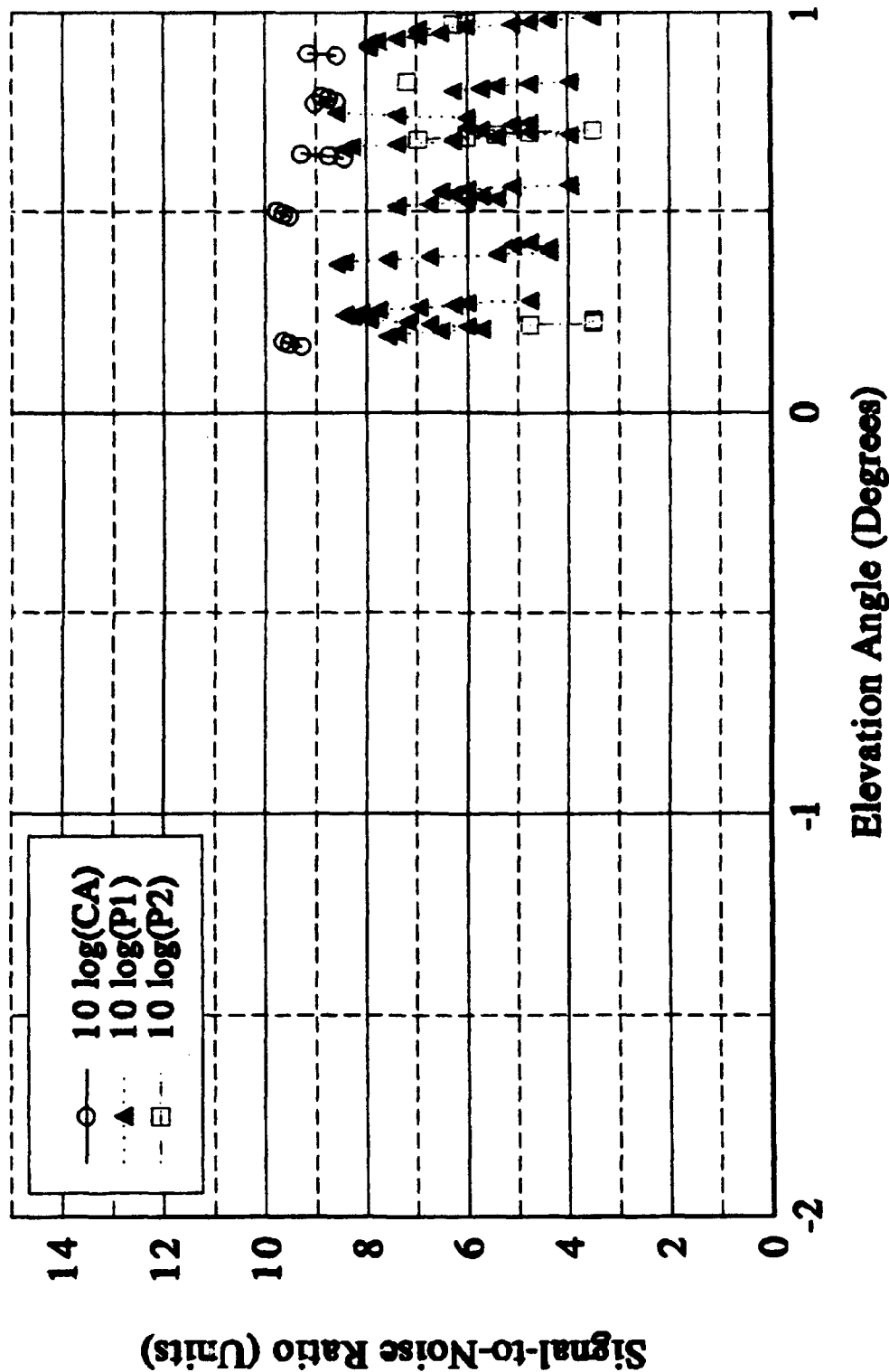- 10 log(CA)
- 10 log(P1)
- 10 log(P2)

Figure 8a.   SNR for satellite 28 rising on 19 August 1993 as measured by the Trimble 4000SSE receiver.

18

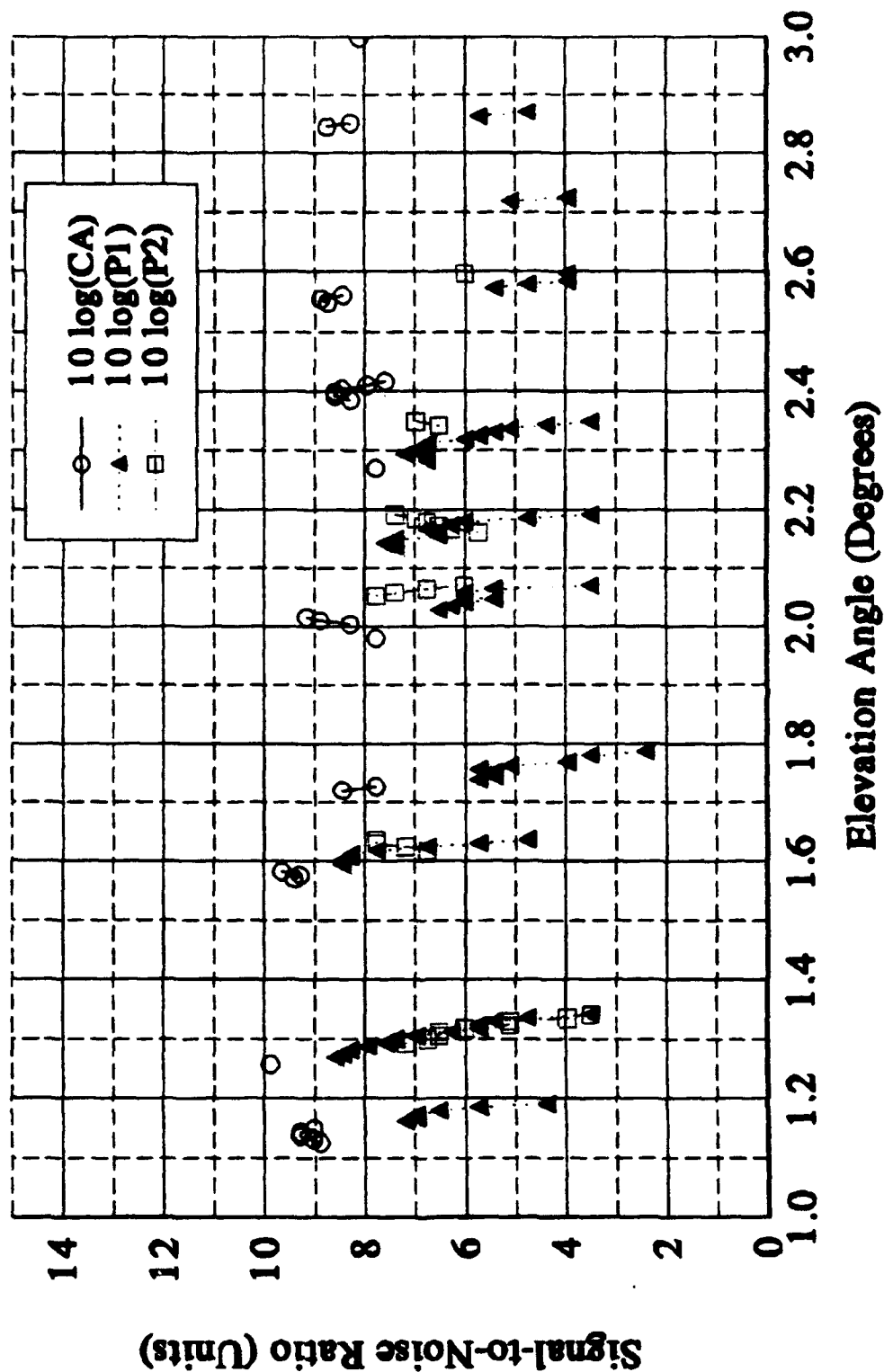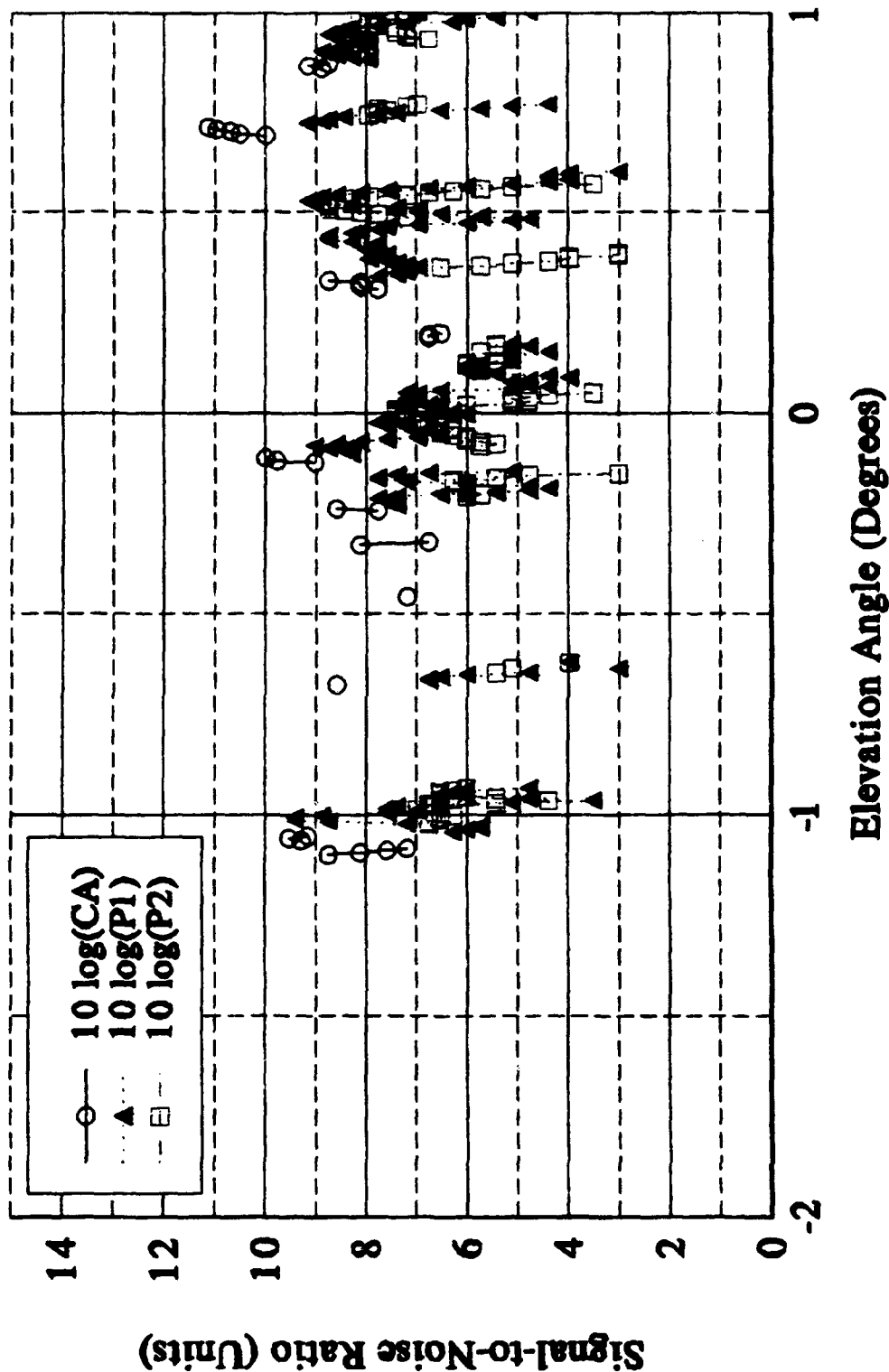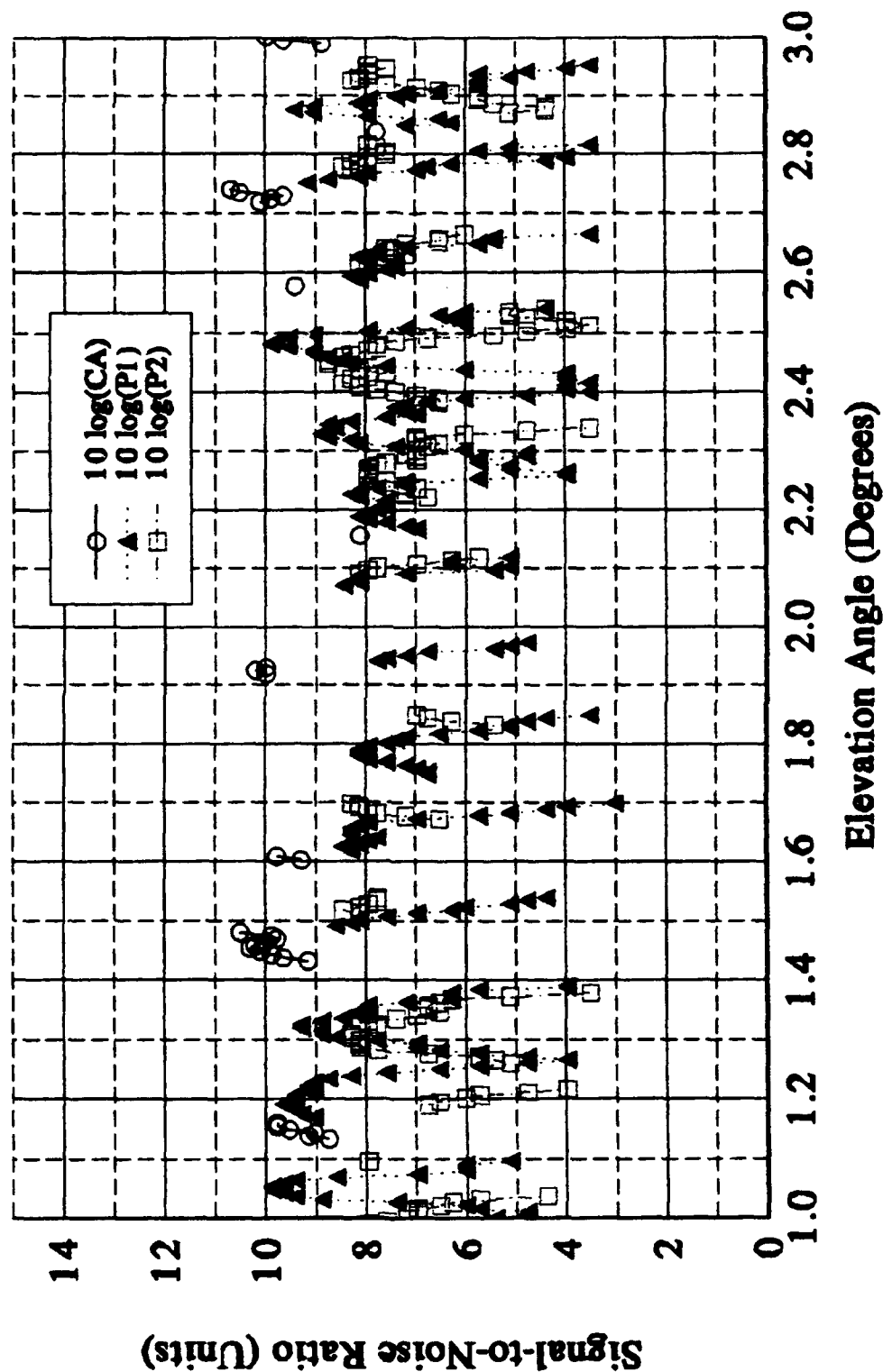**Trimble 4000 SSE**

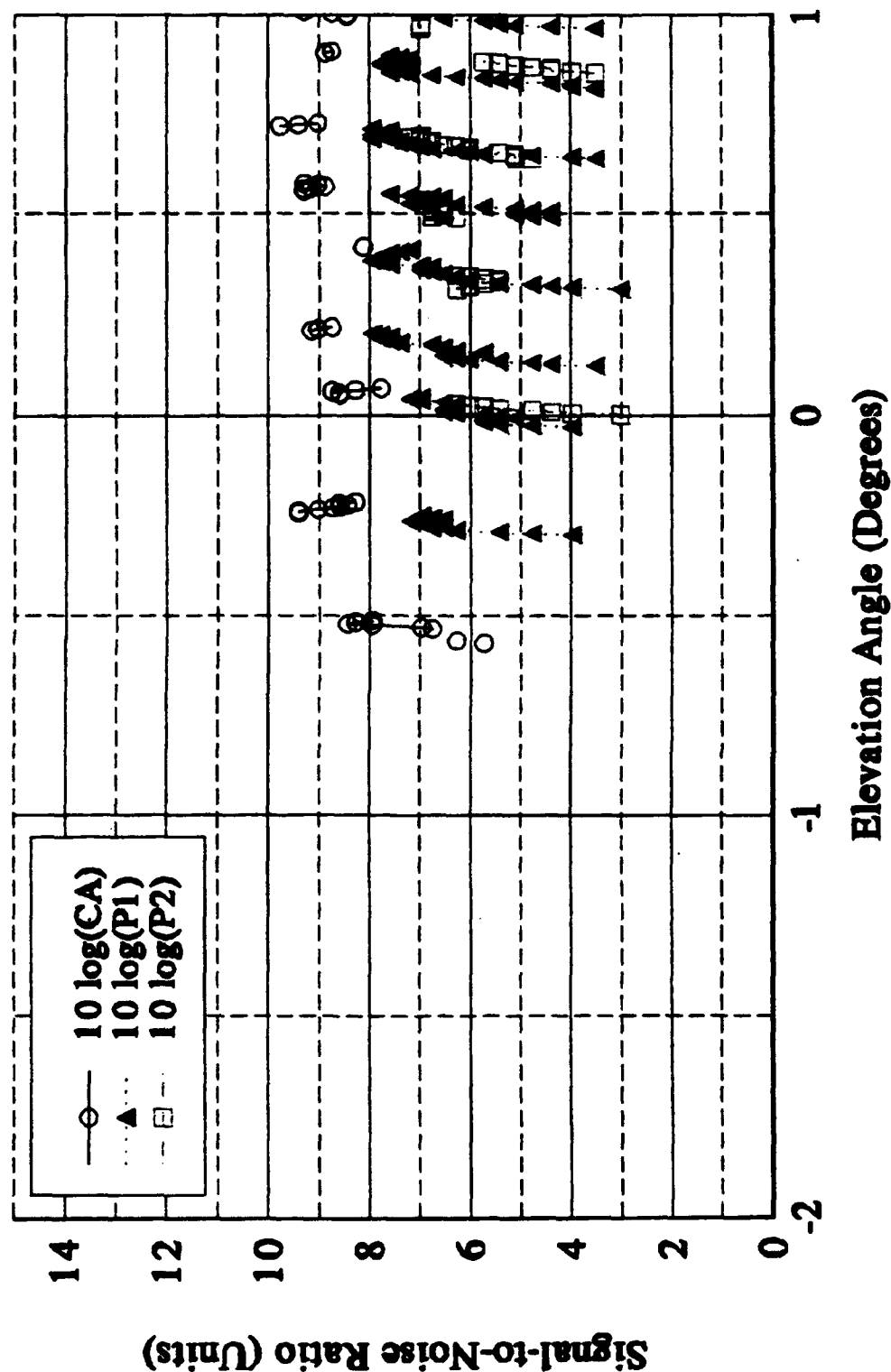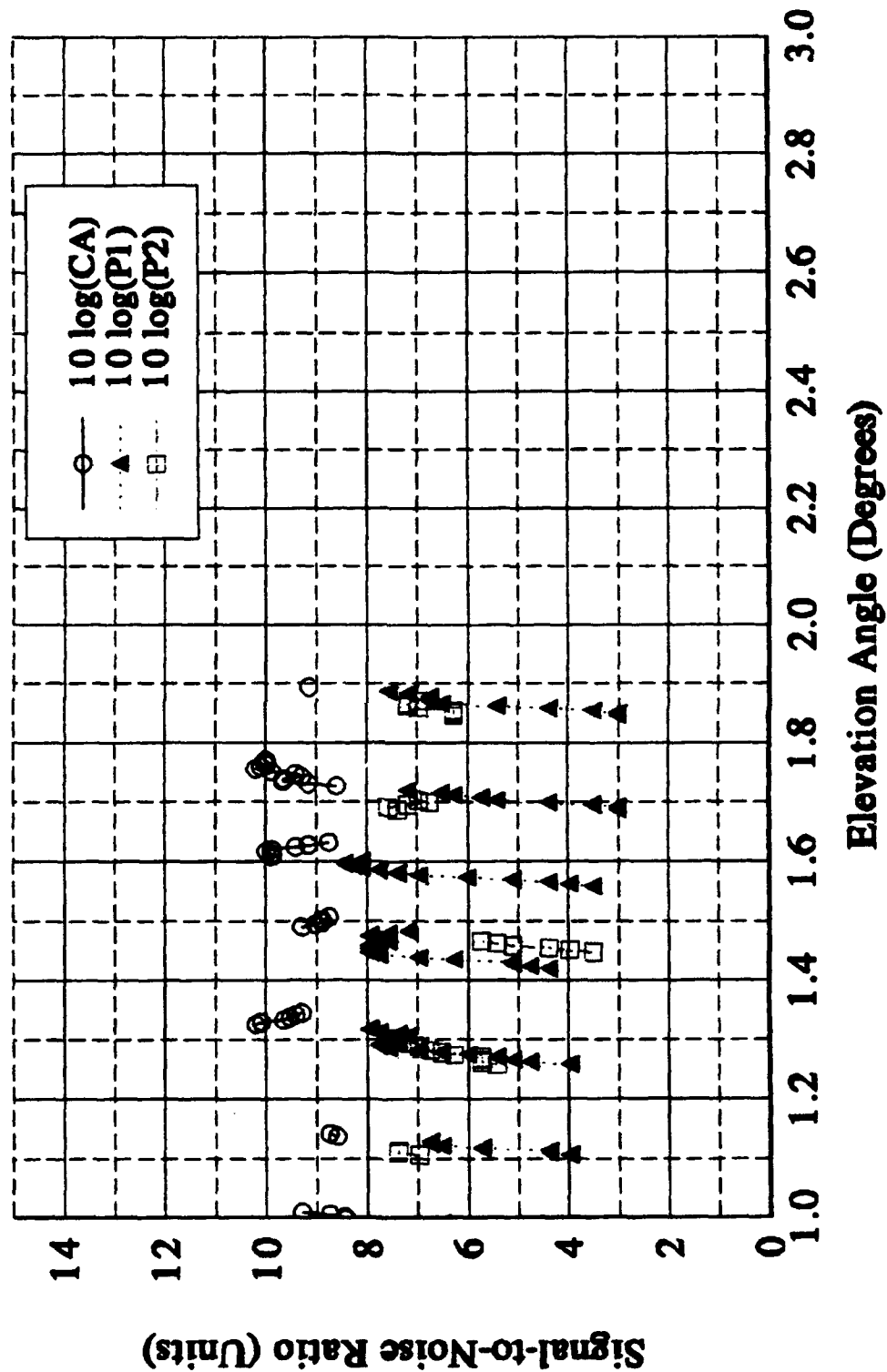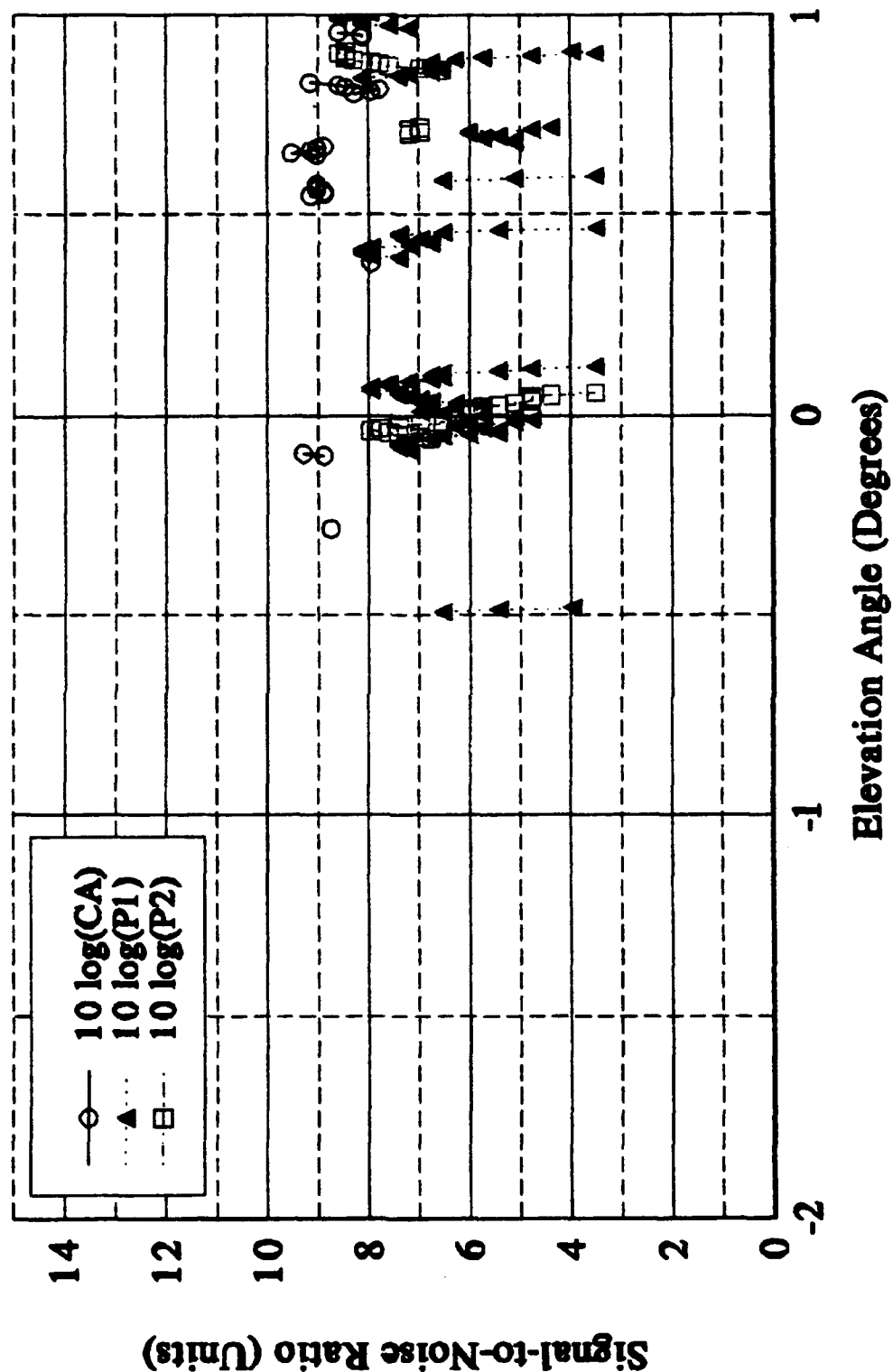**19 August 1993, Satellite 28, 318 Degrees**

Legend:
- 10 log(CA)
- 10 log(P1)
- 10 log(P2)

X-axis: **Elevation Angle (Degrees)**

Y-axis: **Signal-to-Noise Ratio (Units)**

Figure 8b.   SNR for satellite 28 rising on 19 August 1993 as measured by the Trimble 4000SSE receiver (cont'd).

19

Figure 9a. SNR for satellite 20 rising on 19 August 1993 as measured by the Trimble 4000SSE receiver.

Figure 9b.   SNR for satellite 20 rising on 19 August 1993 as measured by the Trimble 4000SSE receiver (cont'd).
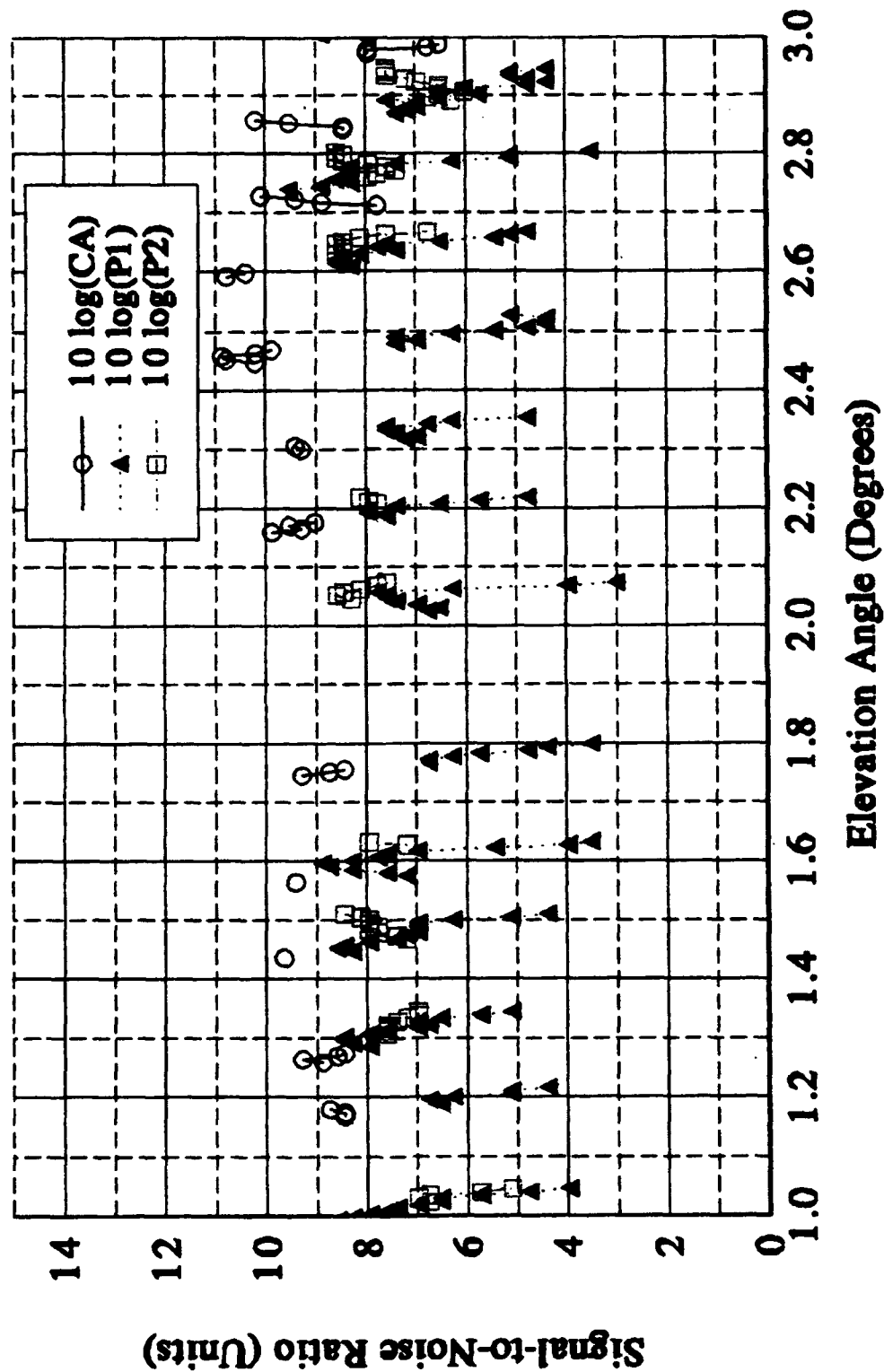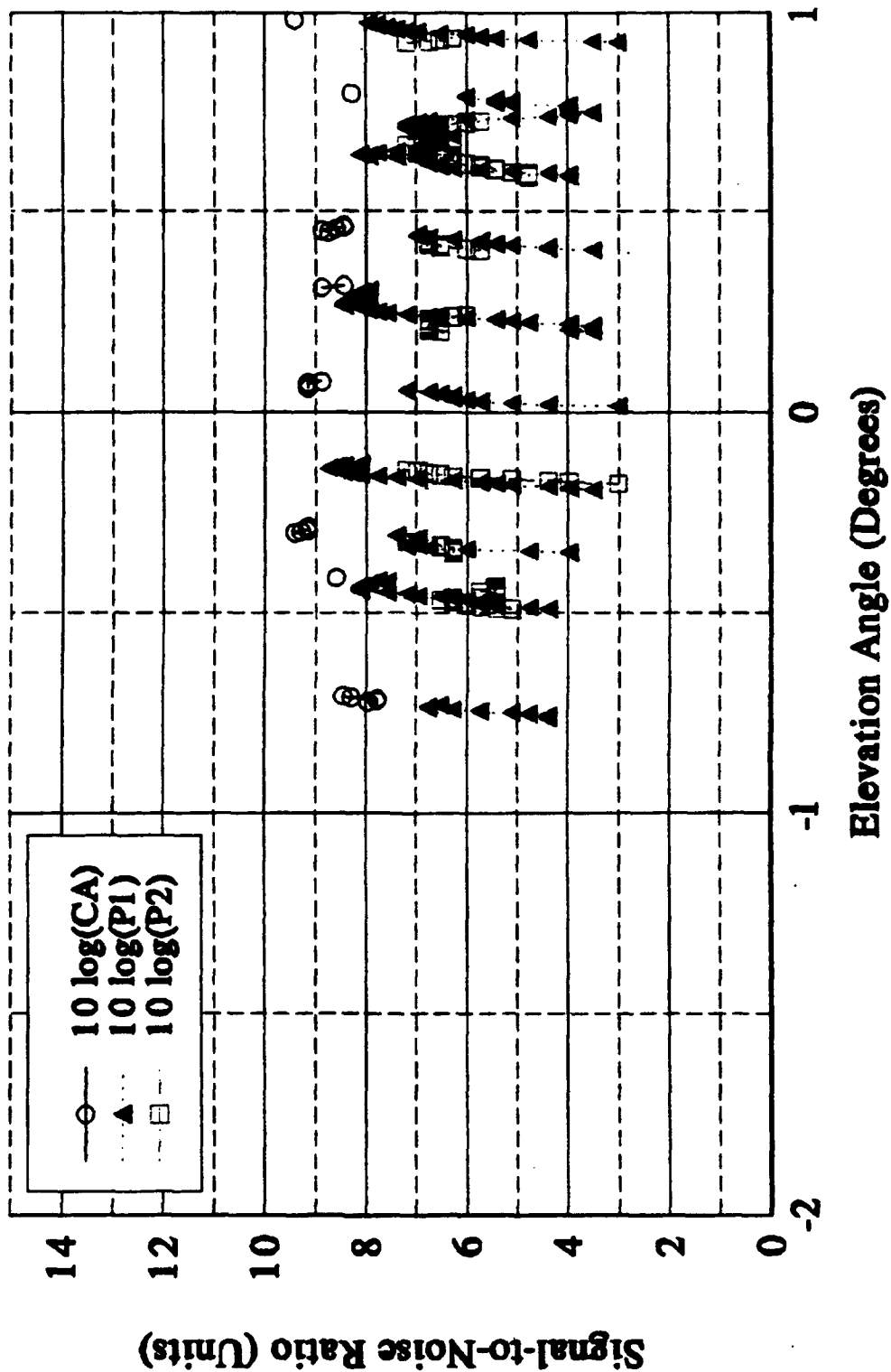
21

Figure 10a.   SNR for satellite 26 setting on 20 August 1993 as measured by the Trimble 4000SSE receiver.

Trimble 4000 SSE

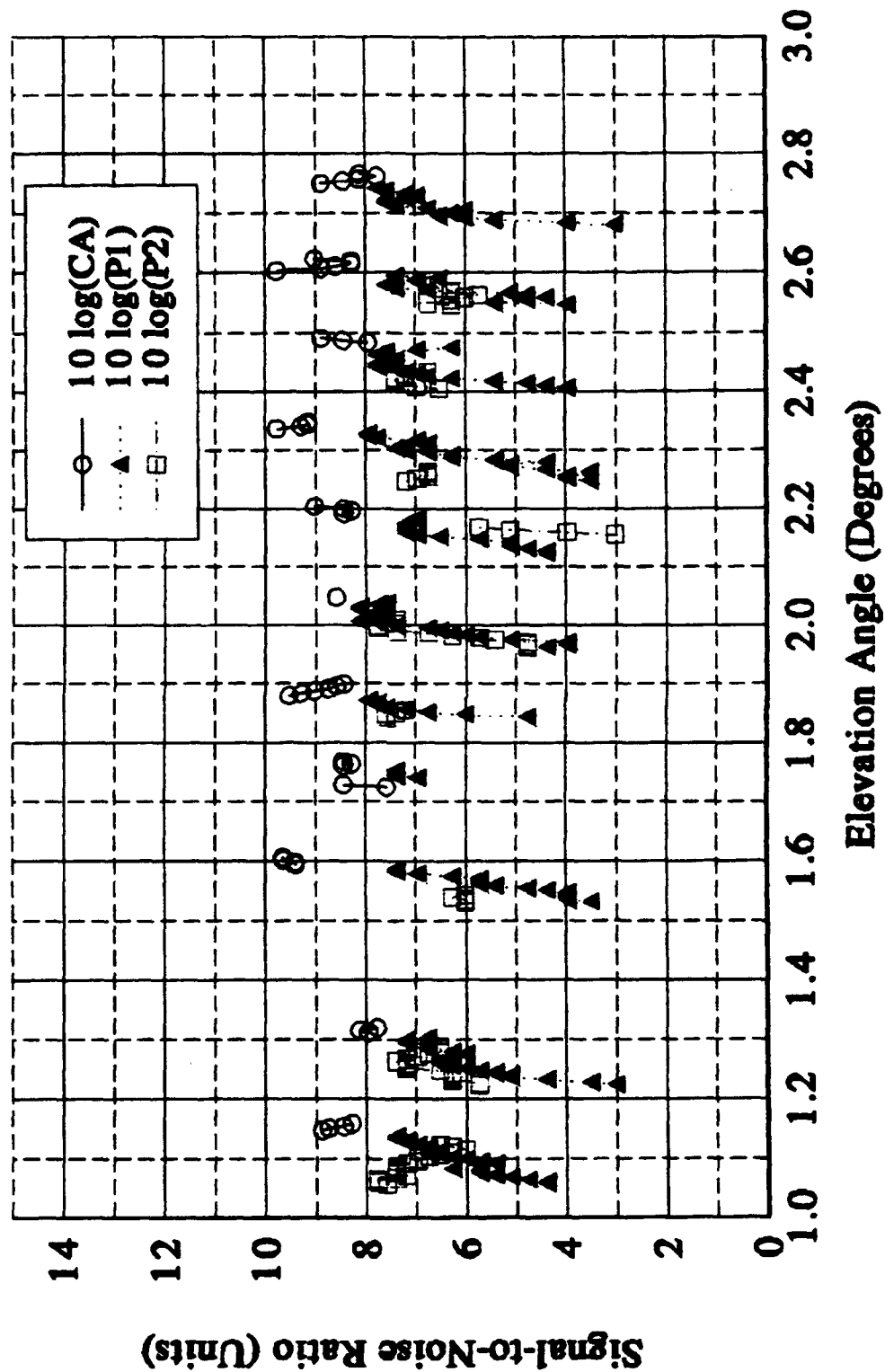**20 August 1993, Satellite 26, 216 Degrees**

Figure 10b. SNR for satellite 26 setting on 20 August 1993 as measured by the Trimble 4000SSE receiver (cont'd).

23

Figure 11a.   SNR for satellite 20 rising on 22 August 1993 as measured by the Trimble 4000SSE receiver.

Figure 11b. SNR for satellite 20 rising on 22 August 1993 as measured by the Trimble 4000SSE receiver (cont'd).

25

Figure 12a. SNR for satellite 26 setting on 22 August 1993 as measured by the Trimble 4000SSE receiver.

Figure 12b. SNR for satellite 26 setting on 22 August 1993 as measured by the Trimble 4000SSE receiver (cont'd).
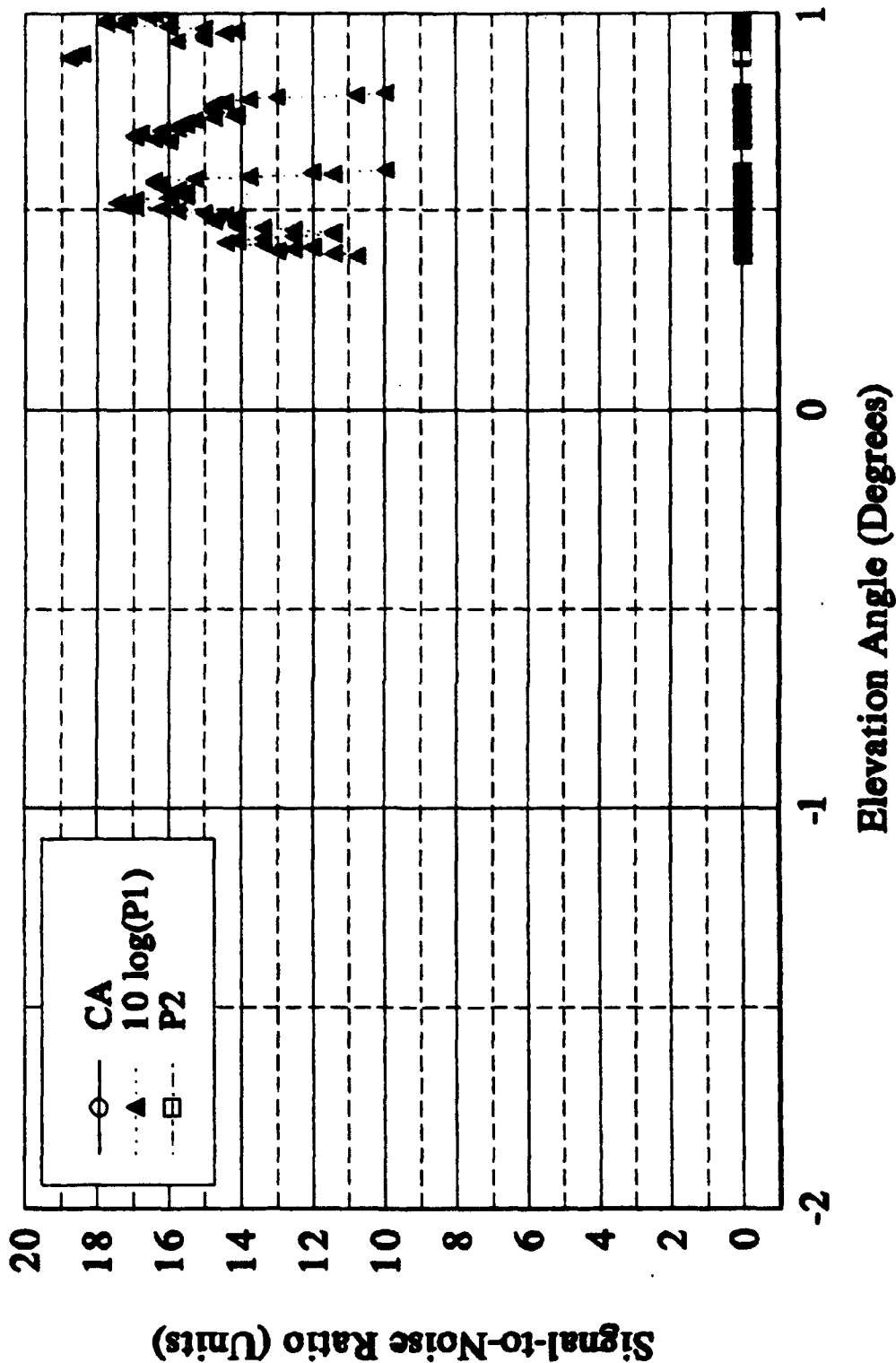
27

Figure 13a. SNR for satellite 20 rising on 25 August 1993 as measured by the Ashtech MD-XII receiver.

28

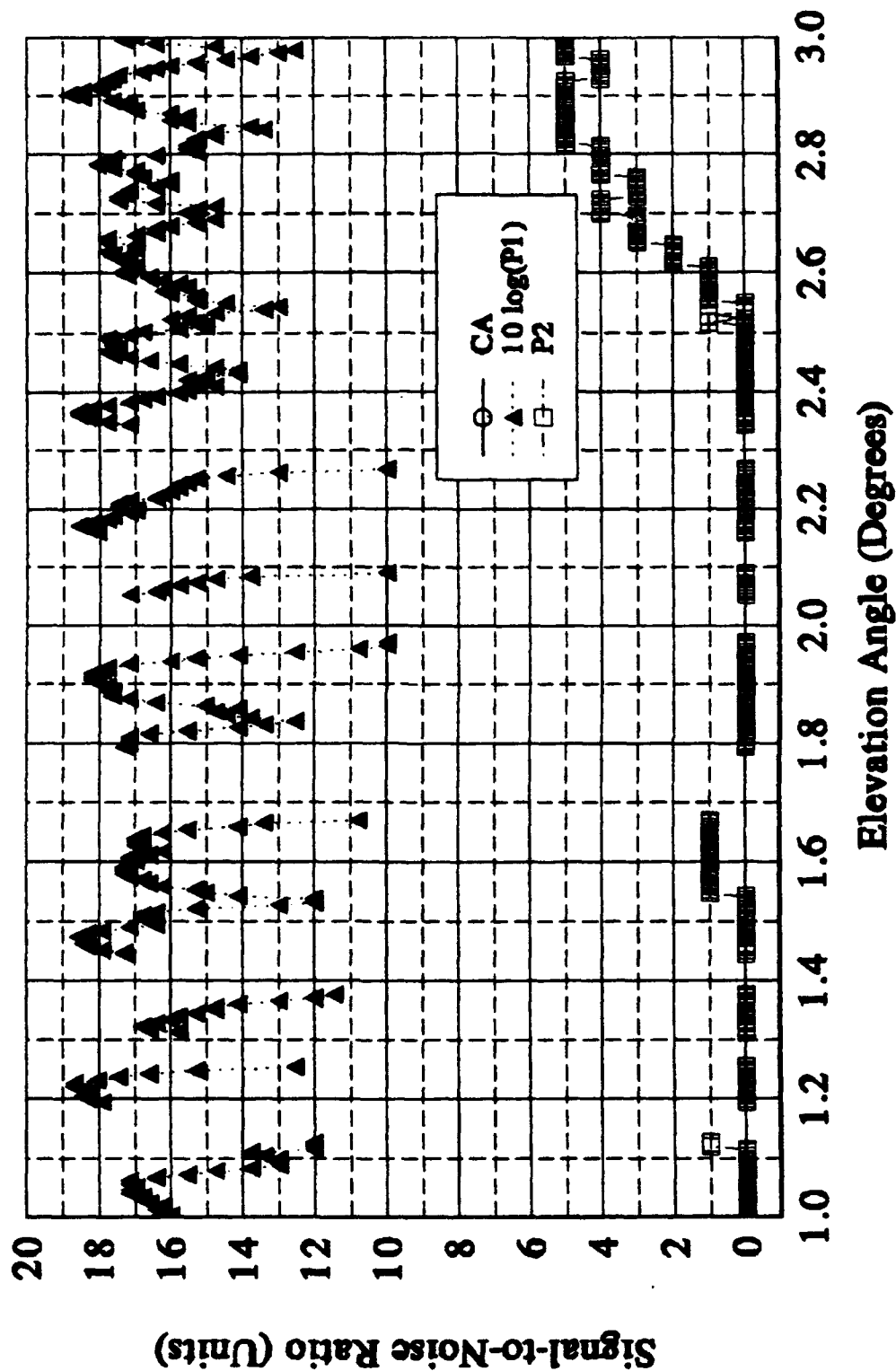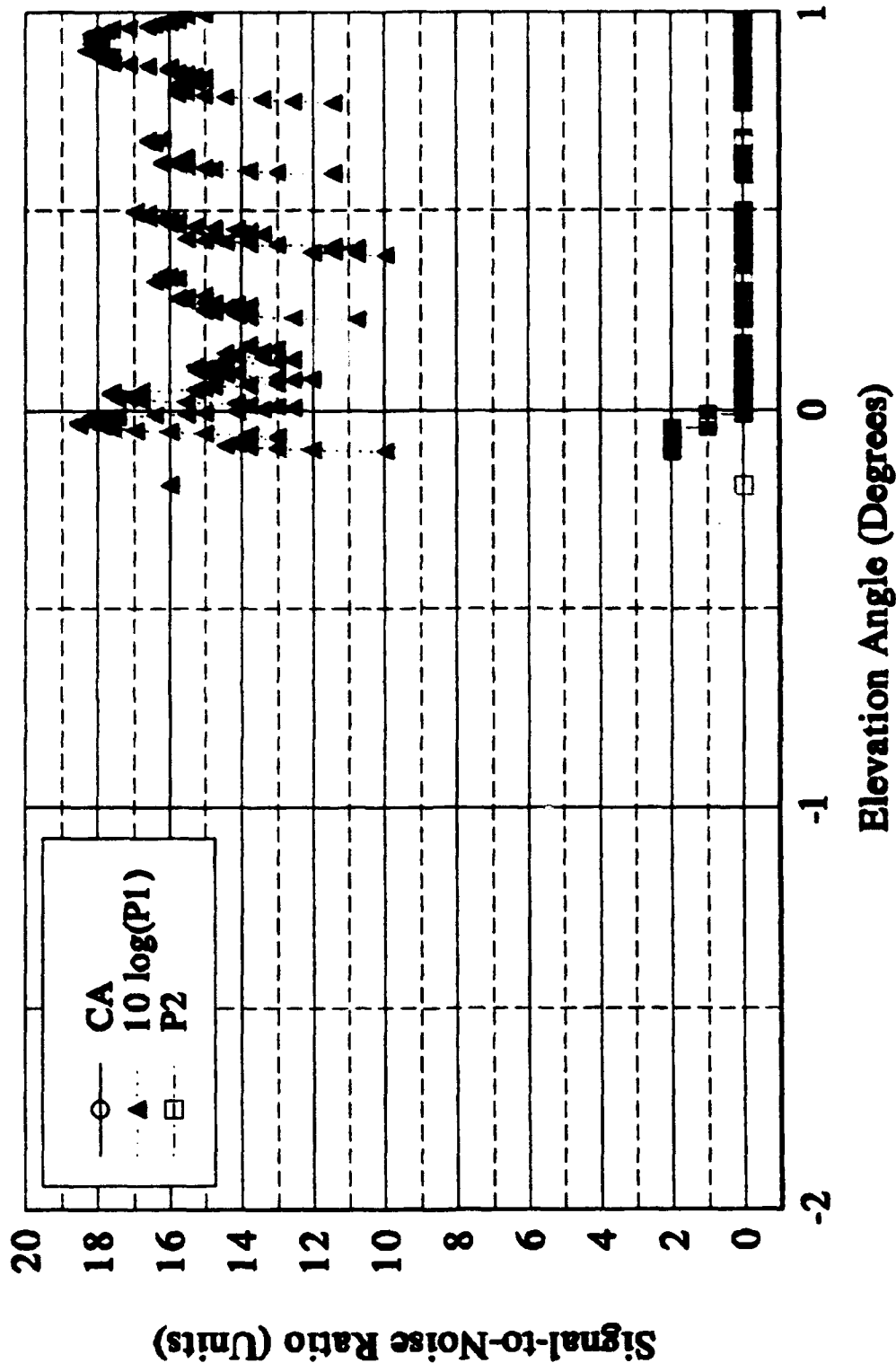**Ashtech MD-XII**

25 August 1993, Satellite 20, 304 Degrees

Figure 13b. SNR for satellite 20 rising on 25 August 1993 as measured by the Ashtech MD-XII receiver (cont'd).

29

Figure 14a.   SNR for satellite 26 setting on 25 August 1993 as measured by the Ashtech MD-XII receiver.

Figure 14b. SNR for satellite 26 setting on 25 August 1993 as measured by the Ashtech MD-XII receiver (cont'd).

31
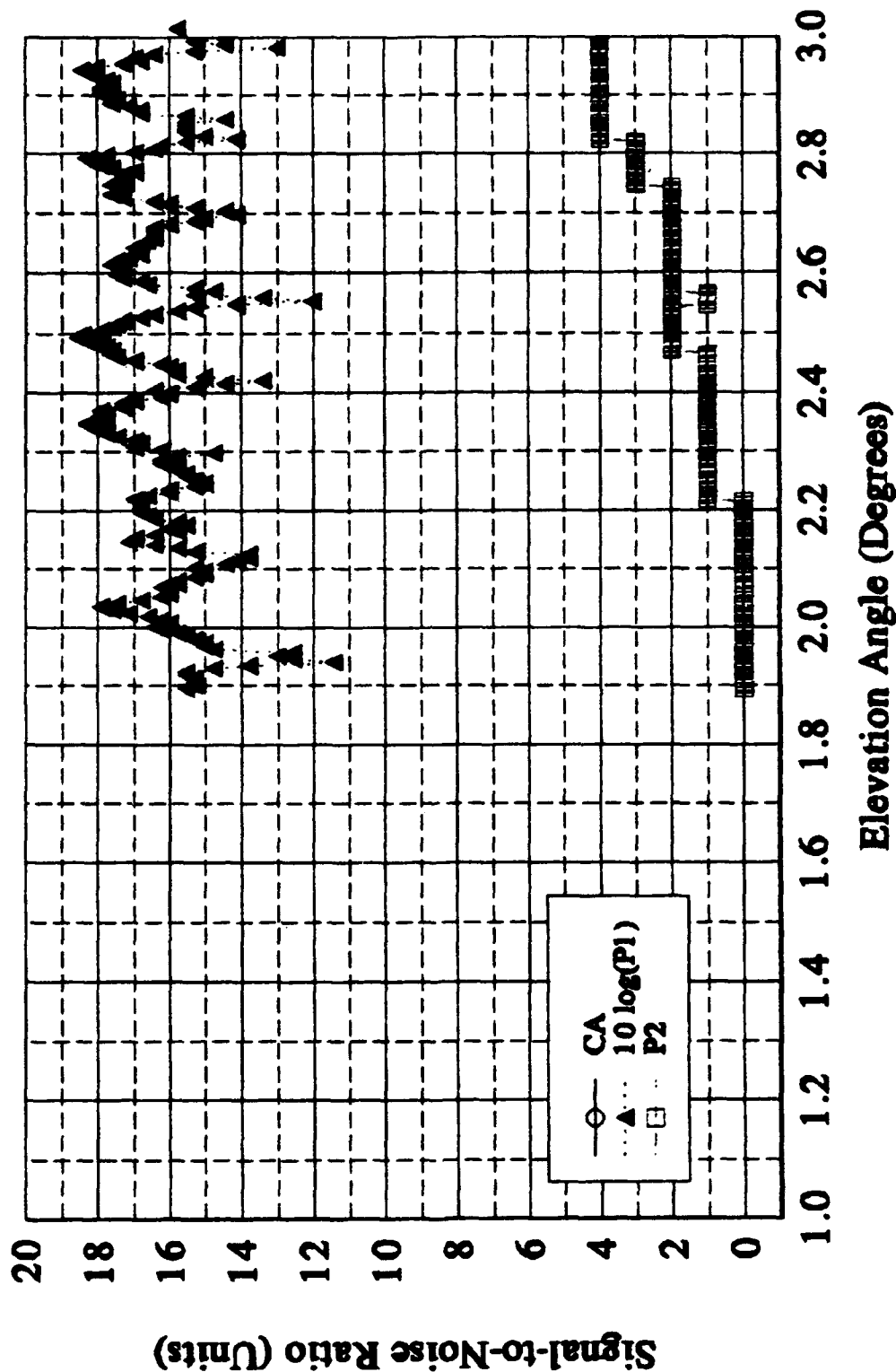
Figure 15. SNR for satellite 22 rising on 25 August 1993 as measured by the Ashtech MD-XII receiver.

Figure 16.   SNR for satellite 23 rising on 25 August 1993 as measured by the Ashtech MD-XII receiver.

33

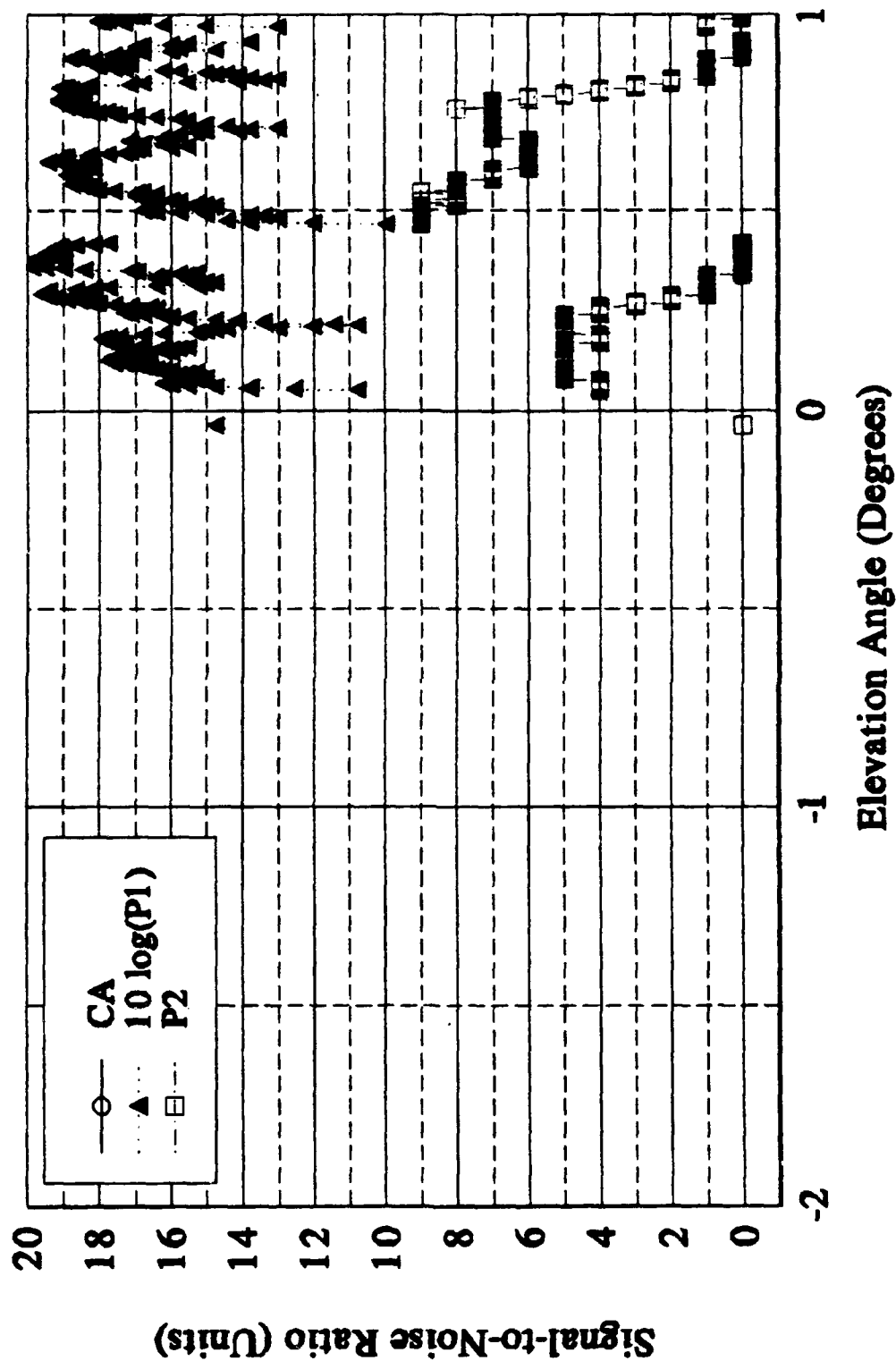Figure 17a.   SNR for satellite 25 setting on 25 August 1993 as measured by the Ashtech MD-XII receiver.
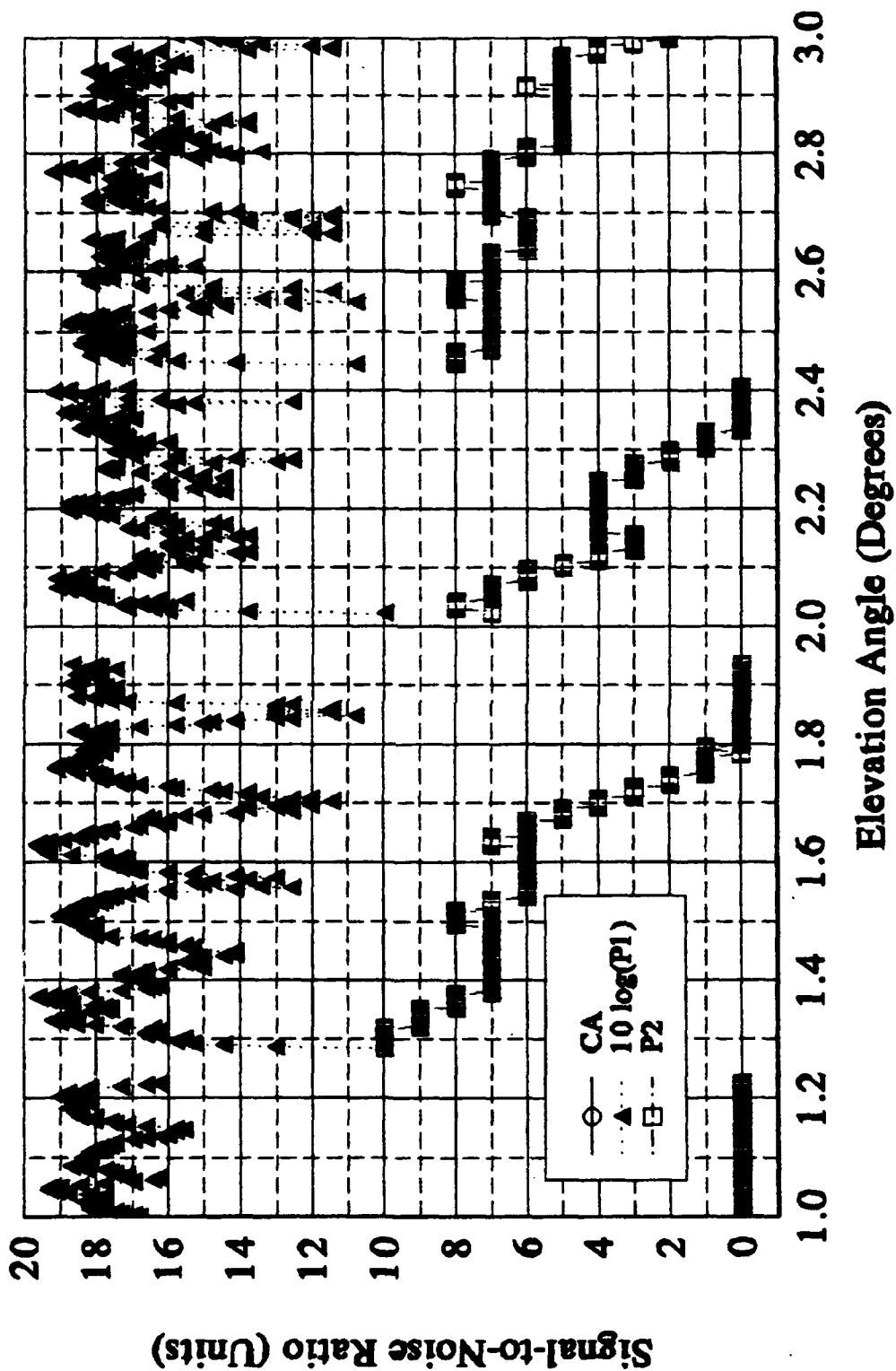
Figure 17b. SNR for satellite 25 setting on 25 August 1993 as measured by the Ashtech MD-XII receiver (cont'd).

35

CONCLUSIONS

Signal-to-noise ratio tests of three high-performance GPS receivers in severe multipath conditions clearly show the Allen Osborne Associates TurboRogue SNR-8000 receiver is superior in locking and tracking C/A, P1, and P2 codes at very low receiver-to-satellite elevation angles. The Trimble 4000 SSE, while ideal for many geodetic applications, loses lock and fails to track at these very low elevation angles. The Ashtech MD XII receiver locks and tracks P1 code reasonably well at elevation angles greater than 0 degree. Its coarse SNR measurement of the P2 code renders this receiver useless for the GPS Sounder application.

Of the three receivers tested, only the AOA is acceptable for use with the GPS Sounder.

REFERENCES

Anderson, K. D. 1982. "Inference of refractivity profiles by satellite-to-ground RF measurements," *Radio Sci.*, vol. 17, no. 3, pp. 653–663 (May-June).

Freehafer, J. E. 1951. "Tropospheric refraction," in *Propagation of Short Radio Waves*, D. E. Kerr, Ed., New York, McGraw-Hill, pp. 9–22.

Hitney, H. V. and J. H. Richter. 1976. "Integrated refractive effects prediction system (IREPS)," *Nav. Eng. J.*, vol. 88, no. 2, pp. 257–262 (April).

Hitney, H. V. 1978. "Means for Determining the refractive index profile of the atmosphere," U. S. Patent 4,093,918 of 6 June.

Hitney, H. V., J. H. Richter, R. A. Pappert, K. D. Anderson, and G. B. Baumgartner, Jr. 1985. "Tropospheric radio propagation assessment," *Proc. IEEE*, vol. 73, no. 2 (February).

Hitney, H. V. 1993. "Modeling tropospheric ducting effects on satellite-to-ground paths," AGARD Conference Proceedings, *Multiple Mechanism Propagation Paths (MMPPs) Their Characterization and Influence on System Design* (October).

Rocken, C., and C. Meertens. 1992. "UNAVCO receiver tests," UNAVCO Memo, (8 November).

REPORT DOCUMENTATION PAGE

1. AGENCY USE ONLY (Leave blank)	2. REPORT DATE	3. REPORT TYPE AND DATES COVERED
	April 1994	Final: October 1993

4. TITLE AND SUBTITLE

AN EVALUATION OF THREE GPS RECEIVERS FOR USE IN THE GPS SOUNDER

5. FUNDING NUMBERS

PE: 0602435N
PROJ: R035S83
SUBPROJ: 54-MPB3 01
AC: DN302216

6. AUTHOR(S)

K. D. Anderson

7. PERFORMING ORGANIZATION NAME(S) AND ADDRESS(ES)

Naval Command, Control and Ocean Surveillance Center (NCCOSC)
RDT&E Division
San Diego, CA 92152–5001

8. PERFORMING ORGANIZATION REPORT NUMBER

TR 1637

9. SPONSORING/MONITORING AGENCY NAME(S) AND ADDRESS(ES)

Office of Naval Research
800 North Quincy Street
Arlington, VA 22217

10. SPONSORING/MONITORING AGENCY REPORT NUMBER

11. SUPPLEMENTARY NOTES

12a. DISTRIBUTION/AVAILABILITY STATEMENT

Approved for public release; distribution is unlimited.

12b. DISTRIBUTION CODE

13. ABSTRACT (Maximum 200 words)

Three high performance, geodetic quality, Global Positioning System (GPS) receivers were tested at the Naval Command, Control and Ocean Surveillance Center RDT&E Division to evaluate their use in supporting the GPS Sounder. These tests are focused on comparisons of the signal-to-noise ratio (SNR) of the GPS signals as the GPS satellite is either rising or setting on the ocean horizon. Of primary interest is the ability of the receiver to lock onto and track the GPS signals when the satellite is at elevation angles of less than 1 degree. This requirement is unique to the GPS Sounder and is one of the most stressful conditions for receiver processing. In most applications, GPS signals are never examined at ground-to-satellite elevation angles of less than about 15 degrees because of multipath effects on signal reception. However, the ability to lock onto and track the GPS signals in the presence of severe multipath conditions is crucial to the success of the GPS Sounder.

14. SUBJECT TERMS

Global Positioning System (GPS)   integrated refractive effects
GPS Sounder   GPS receivers
signal propagation

15. NUMBER OF PAGES

46

16. PRICE CODE

17. SECURITY CLASSIFICATION OF REPORT	18. SECURITY CLASSIFICATION OF THIS PAGE	19. SECURITY CLASSIFICATION OF ABSTRACT	20. LIMITATION OF ABSTRACT
UNCLASSIFIED	UNCLASSIFIED	UNCLASSIFIED	SAME AS REPORT

21a. NAME OF RESPONSIBLE INDIVIDUAL	21b. TELEPHONE (Include Area Code)	21c. OFFICE SYMBOL
K. D. Anderson	(619) 553–1420	Code 543

INITIAL DISTRIBUTION

Code 0012	Patent Counsel	(1)
Code 014	K. J. Campbell	(1)
Code 0274B	Library	(2)
Code 0275	Archive/Stock	(6)
Code 50	H. O. Porter	(1)
Code 54	J. H. Richter	(1)
Code 543	R. A. Paulus	(1)
Code 543	K. D. Anderson	(25)
Code 75	J. E. Griffin	(1)

Defense Technical Information Center
Alexandria, VA 22304–6145   (4)

NCCOSC Washington Liaison Office
Washington, DC 20363–5100

Center for Naval Analyses
Alexandria, VA 22302–0268

Navy Acquisition, Research and Development
      Information Center (NARDIC)
Arlington, VA 22244–5114

GIDEP Operations Center
Corona, CA 91718–8000

NCCOSC Division Detachment
Warminster, PA 18974–5000